THE ASTRONOMICAL JOURNAL, 117:1864–1889, 1999 April

SPECTRAL IRRADIANCE CALIBRATION IN THE INFRARED. X. A SELF-CONSISTENT RADIOMETRIC ALL-SKY NETWORK OF ABSOLUTELY CALIBRATED STELLAR SPECTRA[1]

MARTIN COHEN
Vanguard Research, Inc., Suite 204, 5321 Scotts Valley Drive, Scotts Valley, CA 95066; and Radio Astronomy Laboratory, 601 Campbell Hall, University of California, Berkeley, CA 94720; mcohen@astro.berkeley.edu

RUSSELL G. WALKER
Vanguard Research, Inc., Suite 204, 5321 Scotts Valley Drive, Scotts Valley, CA 95066; russ@vrisv.com

BRIAN CARTER
Carter Observatory, P.O. Box 2909, Wellington, New Zealand; brian.carter@vuw.ac.nz

PETER HAMMERSLEY AND MARK KIDGER
Instituto de Astrofísica de Canarias, Via Lactea, E-38200 La Laguna, Tenerife, Spain; plh@ll.iac.es, mrk@ll.iac.es

AND

KUNIO NOGUCHI
National Astronomical Observatory of Japan, Osawa, Mitaka 181-8588, Japan; knoguchi@optik.mtk.nao.ac.jp
Received 1998 October 15; accepted 1998 December 14

ABSTRACT

We start from our six absolutely calibrated continuous stellar spectra from 1.2 to 35 μm for K0, K1.5, K3, K5, and M0 giants. These were constructed as far as possible from actual observed spectral fragments taken from the ground, the Kuiper Airborne Observatory, and the *IRAS* Low Resolution Spectrometer, and all have a common calibration pedigree. From these we spawn 422 calibrated "spectral templates" for stars with spectral types in the ranges G9.5–K3.5 III and K4.5–M0.5 III. We normalize each template by photometry for the individual stars using published and/or newly secured near- and mid-infrared photometry obtained through fully characterized, absolutely calibrated, combinations of filter passband, detector radiance response, and mean terrestrial atmospheric transmission. These templates continue our ongoing effort to provide an all-sky network of absolutely calibrated, spectrally continuous, stellar standards for general infrared usage, all with a common, traceable calibration heritage. The wavelength coverage is ideal for calibration of many existing and proposed ground-based, airborne, and satellite sensors, particularly low- to moderate-resolution spectrometers. We analyze the statistics of probable uncertainties, in the normalization of these templates to actual photometry, that quantify the confidence with which we can assert that these templates truly represent the individual stars. Each calibrated template provides an angular diameter for that star. These radiometric angular diameters compare very favorably with those directly observed across the range from 1.6 to 21 mas.

Key words: infrared radiation — methods: analytical — stars: late-type — techniques: spectroscopic

1. INTRODUCTION

Several infrared satellites were launched in the period 1995–1996: the joint ISAS/NASA *Infrared Telescope in Space* (*IRTS*; Murakami et al. 1994, 1996), which surveyed about 8% of the sky in 1995; the European Space Agency's *Infrared Space Observatory* (*ISO*; Kessler et al. 1996), with the involvement of the US and Japan; and the US *Midcourse Space Experiment* (*MSX*; Mill et al. 1994), launched in spring 1996. NASA's *Wide Field Infrared Explorer* (*WIRE*) mission is scheduled for a 1999 launch, and SOFIA, the stratospheric observatory project, is fast proceeding. There is an urgent need not only to rationalize IR calibration and place it in a common and well-defined context, but also to provide a network of calibrators well distributed across the sky, with a common, traceable pedigree. This network should be sufficiently dense to have a member relatively close to an arbitrary direction, because satellites and aircraft cannot afford major excursions in pointing to secure measurements of the few traditional calibration objects. Dynamic range, too, is an issue, and such a network should include stars fainter than today's popular "standard" stars.

In the first paper of this series, we described a self-consistent effort to provide absolutely calibrated broad- and narrowband infrared photometry based upon a carefully selected, infrared-customized pair of stellar models for Vega and Sirius, created by R. L. Kurucz and absolutely calibrated by Cohen et al. (1992a, hereafter Paper I). These hot stellar models have been employed as reference spectra to calibrate cool giants by methods detailed by Cohen, Walker, & Witteborn (1992b, hereafter Paper II) and amplified by Cohen et al. (1995, 1996a, 1996b, hereafter Papers IV, VI, and VII). This approach has yielded 12 infrared-bright secondary stellar standards with calibration pedigrees directly traceable to our primary radiometric standard, namely, α CMa. These cool giant spectra are totally unlike any blackbody energy distribution and are dominated by the fundamental absorption and overtones of CO and SiO. These molecular bands are common among cool giants and supergiants (Cohen et al. 1992c, hereafter Paper III). The issue of extrapolation of observed spectra to long wavelengths was also addressed in Papers IV (to 35 μm) and VII (to 300 μm). Paper V discusses the UKIRT CGS3 10/20 μm spectrometer's calibration characteristics

[1] Based on observations made with Telescopio Carlos Sanchez, operated on the island of Tenerife by the Instituto de Astrofísica de Canarias in the Spanish Observatorio del Teide of the Instituto de Astrofísica de Canarias.

because of its central role in the assembly of our composite spectra (Cohen & Davies 1995).

The value of the cool giants, as opposed to A- or G-type dwarfs, is that they can satisfy the need for calibrators over a very broad range of wavelengths and can furnish *empirical* infrared standards for low- and moderate-resolution spectrometers, particularly spaceborne devices. The spectra of warmer stars decline faster with increasing wavelength, limiting their value to the near-infrared for spectroscopy and increasing the reliance on theoretical modeling to interpolate and extrapolate existing infrared spectra.

Papers II, IV, and VII demonstrate the assembly of spectra for the popular infrared calibrators, β Gem (K0 III), α Boo (K1.5 III), α Hya (K3 III), α Tau (K5 III), and β And (M0 III). In the present paper we demonstrate how any such observed spectrum, or "composite," can be used to create many calibrated stellar spectra. Our fundamental assumption is that the dereddened infrared spectrum of any observed K0–M0 giant accurately represents the intrinsic spectrum of any other giant with an identical type as the composite from which the "template" is created. Then all that is needed to constrain the adopted template (spectral shape) for a specific star, spectroscopically unobserved in the infrared, is a measure of its individual interstellar reddening and its infrared photometry (with meaningful errors) in a "well characterized" system of filters. By this we imply that we have digitized versions of their cold transmission profiles and actual, or at least generic, detector responses, and mean atmospheric transmission profiles. These combinations of filter, atmosphere (for ground-based data), and detector responses have been calibrated using our "zero magnitude" Vega spectrum (Paper I).

We emphasize "well characterized" because too often the infrared literature abounds with "magnitudes" without the definition of zero magnitude for each filter, any magnitudes adopted for a stipulated set of "standard stars," a published accessible measurement of the filter transmission profile at its cold operating point, inclusion of the detector's radiance response curve, or any reference to a site-specific terrestrial atmospheric transmission profile. It is sometimes possible to establish "zero-point offsets" (see § 4.2) for random published photometry, but it is generally impossible to trace the separate influences on the magnitudes adopted for several different standards on the cited magnitudes for individual target stars of interest. Further, most infrared "calibration" has consisted of assuming that each distinct "calibrator" can be represented by a blackbody at its effective temperature. As illustrated in this series of papers, this is patently not the case. Worse, the extent of the errors made by the blackbody assumption differs from star to star, even at the same wavelength, rendering most published infrared photometry, and especially spectroscopy, untraceable and, therefore, not rectifiable post facto to any self-consistent calibration framework. It is these reasons that make a fresh approach to infrared stellar calibration desirable, and the needs of three recent infrared satellites during 1995–1998 that render our efforts timely.

It is our philosophy that spectrometers can provide accurate spectral shapes but not necessarily accurate spectrophotometric levels (cf. Papers II, V). This is because one requires identical external conditions (seeing, atmospheric emission and transmission) both for target and reference stars (see Paper V); yet, small apertures and narrow slits prevail. Therefore we find it especially disturbing, in light of the plethora of different infrared photometric systems in the literature and in current usage, that many major observatories have decommissioned their photometers or are seriously contemplating this radical (economically driven) action, in favor of infrared array cameras that not only perpetuate this infelicitous calibration legacy but suffer from their own particular calibration problems and limitations (see, e.g., Glass 1993).

In 1994 October we built a prototype of the network of calibrators described in the current paper. The resulting 183 calibrated templates were provided to the *IRTS*, *ISO*, and *MSX* teams to address at least some of their calibration needs. The new network is more extensive, supported by a greater volume of more precise characterized photometry, and incorporates rigorous tracking of a greater number of sources of uncertainty. In Paper IX of the series, Cohen (1998) describes a pilot study and validation of the template technique applied to space-based (*COBE*/DIRBE) radiometry.

In § 2, we describe the construction of a template from a "composite" observed spectrum and its application to a star with characterized reliable photometry but lacking spectroscopy. The criteria used to select the 573 stars in our proposed radiometric network form the substance of § 3. Section 4 describes the characterized photometry that we have used to create the calibrated templates. New photometry by B. C., P. H., M. K., and K. N., in direct support of this paper, appears in Tables A1–A5 of the Appendix. We also summarize the requisite attributes of these systems, and of all other traceable photometric systems that we have been able to calibrate, from archival cold scanned filter profiles and basis stars. Section 5 tabulates the stars for which we have created calibrated templates, along with a discussion of their qualities and absolute uncertainties. Section 6 explains how to obtain our models, composites, and templates and describes the information that accompanies each to provide traceability in the calibration, and to document the actual processes of composite assembly or template normalization.

2. CREATING TEMPLATES

One fully observed K/M giant spectrum can be used to create many calibrated stellar spectra if one makes the fundamental "template assumption," that the dereddened spectral shape of any observed K0–M0 giant accurately represents the intrinsic spectrum of any other giant with the same two-dimensional MK spectral type as the star from which the "template" is created. To customize the adopted template (i.e., the spectral shape) for a particular star requires photometry of it in a well-characterized system, together with pertinent uncertainties.

Every 1.2–35 μm K/M giant spectrum is dereddened according to its own extinction (actually, all the bright cool giants relevant to the present paper have zero reddening) and lightly smoothed in an information-preserving fashion (Jacobson 1990) that eliminates inappropriate high-frequency noise (i.e., beyond the actual resolution of the spectrometers used for the original observations). Figure 1 illustrates the result of this procedure for the K5 III template derived from the α Tau composite and shows the high-frequency noise that has been removed. The smoothed, intrinsic spectral shapes thereby provide calibrated "spectral templates" for giants of spectral types K0, K1.5, K3, K5, and M0. Specifically, the correspondence between

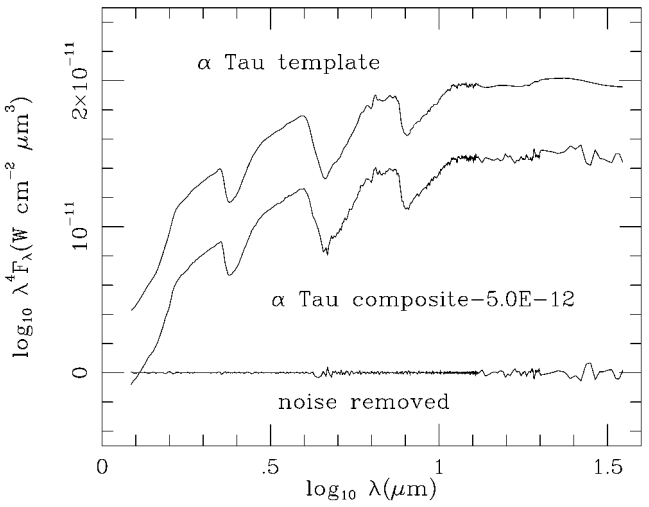

FIG. 1.—Creation of a template from a composite (observed) spectrum. This example, for α Tau, illustrates the result (*top curve*) of lightly smoothing the observed absolute spectrum (*middle curve*; displaced vertically for easier display). Note that, for this star, the extinction is zero, so no dereddening was applied to the composite. The high-frequency "noise" that was filtered away is represented by the lowest curve.

spectral type, template, and the latest published absolute spectrum is as follows: K0, β Gem (Paper IV); K1.5, α Boo (Paper VII); K3, α Hya (Paper IV); K5, α Tau (Paper II); and M0, β And (Paper IV).

The procedure for templating a target star that is spectroscopically unobserved in the IR is to select the appropriate intrinsic template shape, apply reddening according to the target star's extinction [determined from $E(B-V)$], and normalize the resulting reddened template by photometry specific to the star through fully characterized, absolutely calibrated, combinations of detector radiance response, filter passband, and site-specific mean terrestrial atmosphere (if ground-based data) or overall system response functions such as those provided by *IRAS* and DIRBE. The result is a scaled spectral template, with a mean scale factor determined from the set of comparisons of expected in-band fluxes with those actually observed, and an associated uncertainty, assessed from the inverse-variance–weighted set of multipliers for a star (one multiplier and associated uncertainty for each characterized passband used). Each template is as complete in its wavelength coverage as the pristine composite from which it was derived, namely, 1.2–35 μm. No attempt has been made to regrid every composite to a common, or even an equally spaced, wavelength scale, for such an interpolation would spawn yet another set of formal uncertainties. Note that the mean scale factor for a given template is relative to the appropriate composite stellar spectrum, so that two stars with the same scale factor, but made from different spectral templates, will not have the same angular diameter. The angular diameters used for each reference template are those we derived (with appropriate uncertainties) in Paper VII, all of which agree well with direct observations. The derived diameters for newly templated stars are simply the reference templates' diameters multiplied by the square root of the relevant scale factors.

The extinction determination merits discussion. We applied one of three methods for determining A_V to each star templated. Extinctions for an appreciable number of K and M giants are given by McWilliam (1990) or are derivable from the $E(B-V)$ presented by Feast, Whitelock, & Carter (1990). Therefore, the first method was to consult these tabulations and to adopt these authors' estimates of A_V or $E(B-V)$, respectively. For stars not included in their tables, we next estimated a distance to each star, assuming zero extinction and using a recent set of tabulations for M_V (based on work by Gould & Flynn 1992 on K and early M giants). If a star was located within 75 pc of the Sun, we assigned zero extinction on the basis of its location within the local (dust-free) bubble (FitzGerald 1970; Perry & Johnston 1982; Perry, Johnston, & Crawford 1982). Finally, the third method, for stars without tabulated A_V and apparently beyond 75 pc if unreddened, was to compare the observed and intrinsic $B-V$ colors of stars to be templated. Only if $E(B-V)$ exceeded 0.075 did we formally redden the template by $RE(B-V)$ (taking R, the ratio of total to selective extinction, as 3.10; cf. Barlow & Cohen 1977). The allowable range in $B-V$ was obtained by halving J.-C. Mermilliod's (1993, private communication) estimate of the natural dispersion observed among unreddened stars of any given type (taken from his UBV archives; e.g., Mermilliod 1994). For all stars found to have values of $A_V \leq 0.044$ by any of these three techniques, we applied no reddening because the effect of this would yield less than a 1% change in the template at 1.0 μm, and even less at our longer wavelengths. Overall, between the three techniques, 339 stars were assigned zero extinction. Our extinction law was taken to be that used in the SKY model (see Wainscoat et al. 1992).

3. THE PROPOSED RADIOMETRIC NETWORK OF STARS

3.1. *Requirements*

We have assembled a list of candidate calibration objects based on their infrared brightness, degree of variability, complexity of spectrum, and isolation from nearby confusing sources. Our goal was to identify one such source per 50 deg^2 of the sky, leading to a total of about 825 stars. The candidate calibration objects were selected from the *IRAS* Point Source Catalog (1988, hereafter PSC), their nearby point-source and extended neighbors extracted, and the astronomical literature subsequently searched for additional associations, spectral types, luminosity classes, variability data, and spectrometric and photometric observations.

3.2. *Selection Criteria and Procedure*

Candidate calibration stars must conform to the following criteria (Walker & Cohen 1992), listed in the order that they were applied to our search of the *IRAS* database:

1. The candidate sources were required to have high-quality *IRAS* flux measurements at 12 and 25 μm, and the limiting flux had to be consistent with achieving the desired source density (1 source per 50 deg^2) in the final list. The infrared point-source sky model SKY (Wainscoat et al. 1992; Cohen 1994) was used to estimate the density of K0 to M0 giants at the Galactic pole as a function of the limiting flux. It was found that inclusion of all stars with $F_{25} > 1$ Jy would satisfy the surface density requirement (where F_{25} is the *IRAS* PSC flux at 25 μm).

2. The sources had to be normal stars as defined by their location in the infrared color-color diagram. Walker & Cohen (1988) found that normal stars are confined to the

TABLE 1

SPECTRAL TYPE BREAKDOWN OF THE NETWORK OF STARS AND TEMPLATES

Spectral Types	Number of Stars	Number of Templates
All A types	10	0
All F types	11	0
G0, G1 all classes	4	0
G4 III	1	0
G5 II, III, IV	9	0
G6, G6.5 II, III	4	0
G7, G7.5 II, III	6	0
G8, G8.5 II, III, IV	25	0
G9, G9.5 III	21	4
K0, K0.5 II, III, IV	47	46
K1, K1.5 II, III	37	36
K2, K2.5 II, III, IV	64	64
K3, K3.5 II, III	72	71
K4, K4.5 III	68	13
K5, K5.5 II, III	103	101
K6 III	5	5
K7 III	4	4
K8 III	1	1
M0, M0.5 II, III	79	77
M1.5, M2.5 II, III	2	0
Total all types	573	422

$[12]-[25] \leq 0.3$, $[25]-[60] \leq 0.3$ region of the *IRAS* (12, 25, 60) μm color plane, so we required that the flux ratio $F_{12}/F_{25} \geq 3.19$ and, if the star had a high-quality measurement at 60 μm (not required of all stars), the ratio $F_{25}/F_{60} \geq 4.28$.

A search of the PSC for sources that satisfied both criteria 1 and 2 produced 3331 stars. This subset of the PSC served as our database for further suitability tests.

3. As a further assurance of stellar "normality," we required that there be an *IRAS* association for the object and that the associated object be stellar, and not listed as a variable star, emission-line object, or carbon star. We also demanded that the *IRAS* measurements indicate that the probability that the star is variable be less than 90%. Thirty-seven sources were not stellar; 534 were optically known variables, emission-line objects, or carbon stars; and *IRAS* found 44 to be variable.

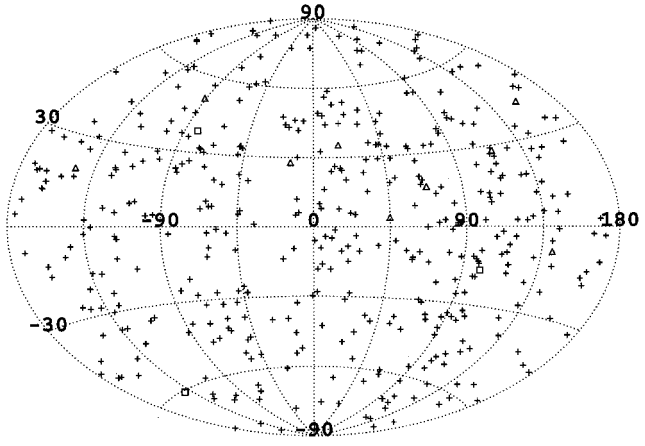

FIG. 2.—Sky distribution of stars in the radiometric network. Squares denote spectra represented by adopted calibrated Kurucz models. Triangles are for low-resolution composites (bright K/M giants). Crosses are the 422 stars in the new fainter network. Coordinates are B1950.0 right ascension and declination, in degrees.

4. To ensure precise photometry, each star must be isolated from other sources that might contribute flux within the field of view of a sensor. We required that the total flux from all known (i.e., cataloged) sources within a radius of 6′ of each network star be less than 5% of the flux at 12 and 25 μm from the potential calibrator; 662 sources failed this test, most of them located near the Galactic plane, or in the Magellanic Clouds, or along the line of sight to the Magellanic Clouds.

5. To further ensure precise photometry, the star should not lie in a field of bright extended infrared emission. Here we demanded that the star not be associated by *IRAS* with a small extended source at either 12 or 25 μm and that the emission at 12 μm due to infrared cirrus in the field (as determined by the PSC's CIRR3, 60 μm indicator) be less than 5% of the source's flux. The actual test applied is $\mathrm{CIRR3} < 6.3F_{12}$, based on our extrapolation of the mean cirrus emission spectrum from 60 to 12 μm, on consideration of the *IRAS* detectors' fields of view and of the apertures and pixel sizes used by these recent infrared satellites. Two hundred forty-four sources failed the small extended source test, and 1451 failed to meet the infrared cirrus criterion. These rejected sources tend to be concentrated in a broad band about the Galactic plane; however, there is a significant high-latitude population.

6. Finally, we restricted our selection of calibration candidates to spectral types A0–M0 and luminosity classes II–IV (for K–M types) or III–V (for A–G), although stars were retained at this stage even if no luminosity class was available. This restriction was intended to limit the influence of molecular absorptions on the photospheric spectrum, and of excess emission due to either dust shells or free-free emission from stellar winds. (We emphasize this latter point in light of the fact that previous compendia of infrared "standard stars" have included a surprising number of supergiants. In our opinion, this risks including spectral energy distributions that are wind dominated, not photospheric, in the near- and mid-infrared, even among non–M-type supergiants.) Since *IRAS* detects late spectral types most efficiently, it is no surprise that 1742 stars failed these spectral constraints, including those stars for which no spectral type was found.

By cutting off our sample at type M0 we also greatly reduce the possibility of significant variability among the candidate stars. Eyer & Grenon (1997) have plotted the variability of stars across the Hertzsprung-Russell diagram. Their data demonstrate that one can select stars as late as M3 III and yet still not exceed 0.04 mag amplitude of variability in the *Hipparcos* band. K giants are usually not characterized by variability (Stebbins & Huffer 1930). In a recent study of 25% of the over 200 K giants named as known, or suspected, variables in the Yale Catalogue of Bright Stars, Percy (1993) found only two stars to be clearly variable in B and/or V. Both are in our atlas, and both showed visible amplitudes of 0.05 mag on a timescale of order 1 month. In each case, all their precision near-infrared photometric points lie on the template curves, and their *IRAS* points are either on the template (31 Lyn = IRAS 08194+4320, K4.5 III) or well within 2 σ of it (AW CVn = IRAS 13495+3441); i.e., we can see no clear evidence in the infrared for problems of variability or noncontemporaneous photometry in these two stars.

TABLE 2

CALIBRATION OF THE PHOTOMETRY SYSTEMS SUPPORTING THIS WORK

System	Filter	In-Band Flux (W cm^{-2})	In-Band Uncertainty (W cm^{-2})	Bandwidth (μm)	F_λ(iso) (W cm^{-2} μm^{-1})	λ_{iso} (μm)
Bessell-Brett	BB H	0.3198E−13	0.6190E−15	0.2799E+00	0.1143E−12	1.658
	BB K	0.1432E−13	0.2627E−15	0.3613E+00	0.3962E−13	2.204
	BB L	0.3198E−14	0.6208E−16	0.4474E+00	0.7148E−14	3.473
	BB L'	0.2552E−14	0.4950E−16	0.5160E+00	0.4945E−14	3.825
	BB M	0.8579E−15	0.1641E−16	0.4057E+00	0.2114E−14	4.764
DIRBE	Band 2	0.1419E−13	0.2536E−15	0.3640E+00	0.3899E−13	2.214
	Band 3	0.6256E−14	0.1051E−15	0.9086E+00	0.6886E−14	3.507
	Band 4	0.1267E−14	0.2343E−16	0.6561E+00	0.1931E−14	4.877
	Band 5	0.4240E−15	0.6782E−17	0.6560E+01	0.6464E−16	11.58
	Band 6	0.5105E−16	0.9166E−18	0.7238E+01	0.7053E−17	20.22
ESO	ESO H	0.2478E−13	0.4271E−15	0.2154E+00	0.1150E−12	1.654
	ESO K	0.1366E−13	0.2277E−15	0.3393E+00	0.4027E−13	2.195
	ESO L	0.3044E−14	0.5163E−16	0.5934E+00	0.5130E−14	3.787
	ESO M	0.7378E−15	0.1490E−16	0.3388E+00	0.2177E−14	4.728
	ESO N	0.4422E−15	0.7273E−17	0.4036E+01	0.1096E−15	10.14
	ESO $N1$	0.1898E−15	0.3856E−17	0.8270E+00	0.2295E−15	8.405
	ESO $N2$	0.1390E−15	0.2816E−17	0.1087E+01	0.1278E−15	9.750
	ESO $N3$	0.5691E−16	0.1252E−17	0.1212E+01	0.4696E−16	12.55
	ESO Q	0.1737E−16	0.3717E−18	0.1591E+01	0.1092E−16	18.12
GBPP	ESOKP H	0.2504E−13	0.4195E−15	0.2197E+00	0.1140E−12	1.659
	ESOKP H_0	0.4211E−14	0.8613E−16	0.3307E−01	0.1273E−12	1.605
	ESOKP K	0.1311E−13	0.2129E−15	0.3294E+00	0.3981E−13	2.202
	ESOKP K_0	0.1566E−14	0.3046E−16	0.4064E−01	0.3853E−13	2.221
	ESOKP L'	0.2943E−14	0.4857E−16	0.5774E+00	0.5097E−14	3.794
	ESOKP L_0	0.2923E−15	0.7230E−17	0.5321E−01	0.5494E−14	3.717
	ESOKP M	0.6911E−15	0.1218E−16	0.3182E+00	0.2172E−14	4.731
	ESOKP N_1	0.1457E−15	0.2801E−17	0.6163E+00	0.2364E−15	8.341
	ESOKP N_2	0.1529E−15	0.2805E−17	0.1174E+01	0.1302E−15	9.703
	ESOKP N_3	0.4068E−16	0.8564E−18	0.9467E+00	0.4297E−16	12.84
IRAS	12 μm	0.5402E−15	0.1124E−16	0.6067E+01	0.8905E−16	10.70
	25 μm	0.4583E−16	0.8213E−18	0.1002E+02	0.4575E−17	22.54
IRC	BB K	0.1432E−13	0.1599E−15	0.3613E+00	0.3962E−13	2.204
IRTF (GBPP)	8.7 μm	0.1547E−15	0.3037E−17	0.8044E+00	0.1924E−15	8.789
	9.8 μm	0.8895E−16	0.1793E−17	0.7242E+00	0.1228E−15	9.847
	12.5 μm	0.5177E−16	0.1119E−17	0.1068E+01	0.4847E−16	12.45
IRTF	N	0.4199E−15	0.6908E−17	0.4360E+01	0.9632E−16	10.47
	Q	0.3580E−16	0.7727E−18	0.4985E+01	0.7182E−17	20.13
KPNO	OTTO H	0.3133E−13	0.5366E−15	0.2735E+00	0.1146E−12	1.656
	OTTO K	0.1266E−13	0.2084E−15	0.3274E+00	0.3866E−13	2.219
	OTTO L	0.2845E−14	0.4586E−16	0.4044E+00	0.7035E−14	3.488
	OTTO M	0.5140E−15	0.9630E−17	0.2256E+00	0.2278E−14	4.672
A. McWilliam	2.17 μm	0.3846E−14	0.6594E−16	0.9239E−01	0.4163E−13	2.175
	2.40 μm	0.2103E−14	0.3745E−16	0.7397E−01	0.2843E−13	2.409
K. N.	Xinglong H	0.2740E−13	0.4170E−15	0.2367E+00	0.1158E−12	1.651
	Xinglong K	0.1271E−13	0.1968E−15	0.3187E+00	0.3988E−13	2.200
	Xinglong L	0.2901E−14	0.4626E−16	0.5669E+00	0.5116E−14	3.790
	ISAS H	0.2760E−13	0.4202E−15	0.2382E+00	0.1159E−12	1.651
	ISAS K	0.1265E−13	0.1959E−15	0.3170E+00	0.3991E−13	2.200
	ISAS L	0.2877E−14	0.4587E−16	0.5629E+00	0.5110E−14	3.791
SAAO	SA H	0.3319E−13	0.6557E−15	0.2893E+00	0.1147E−12	1.655
	SA K	0.1495E−13	0.2910E−15	0.3854E+00	0.3878E−13	2.218
	SA L	0.4096E−14	0.7294E−16	0.5480E+00	0.7475E−14	3.433
M. J. Selby	Kn	0.2155E−14	0.4648E−16	0.5471E−01	0.3938E−13	2.208
	Ln	0.7324E−15	0.1553E−16	0.1416E+00	0.5172E−14	3.779
Tenerife	TCS H	0.2626E−13	0.4359E−15	0.2311E+00	0.1137E−12	1.660
	TCS K	0.1347E−13	0.2223E−15	0.3208E+00	0.4199E−13	2.170
	TCS L'	0.3074E−14	0.5247E−16	0.5298E+00	0.5802E−14	3.668
UKIRT	H	0.2950E−13	0.4475E−15	0.2563E+00	0.1151E−12	1.654
	K	0.1412E−13	0.2163E−15	0.3413E+00	0.4136E−13	2.179
	L	0.3290E−14	0.5259E−16	0.4976E+00	0.6610E−14	3.544
	L'	0.2980E−14	0.4768E−16	0.5664E+00	0.5261E−14	3.761
	M	0.7978E−15	0.1377E−16	0.3790E+00	0.2105E−14	4.770
	N	0.4199E−15	0.6908E−17	0.4360E+01	0.9632E−16	10.47
	8.65 μm	0.2108E−15	0.3891E−17	0.1078E+01	0.1955E−15	8.753
	11.5 μm	0.7065E−16	0.1448E−17	0.1120E+01	0.6308E−16	11.65
	Q	0.3580E−16	0.7727E−18	0.4985E+01	0.7182E−17	20.13

TABLE 2—*Continued*

System	Filter	In-Band Flux (W cm^{-2})	In-Band Uncertainty (W cm^{-2})	Bandwidth (μm)	F_λ(iso) (W cm^{-2} μm^{-1})	λ_{iso} (μm)
WIRO.....	*L*	0.4540E−14	0.6959E−16	0.6528E+00	0.6955E−14	3.474
	M	0.6424E−15	0.1193E−16	0.3644E+00	0.1763E−14	4.990
	8.7 μm	0.1770E−15	0.3412E−17	0.8751E+00	0.2023E−15	8.678
	N	0.4280E−15	0.7177E−17	0.3155E+01	0.1357E−15	9.603
	11.4 μm	0.1291E−15	0.2391E−17	0.1750E+01	0.7376E−16	11.20
	12.6 μm	0.3512E−16	0.8174E−18	0.7648E+00	0.4592E−16	12.62

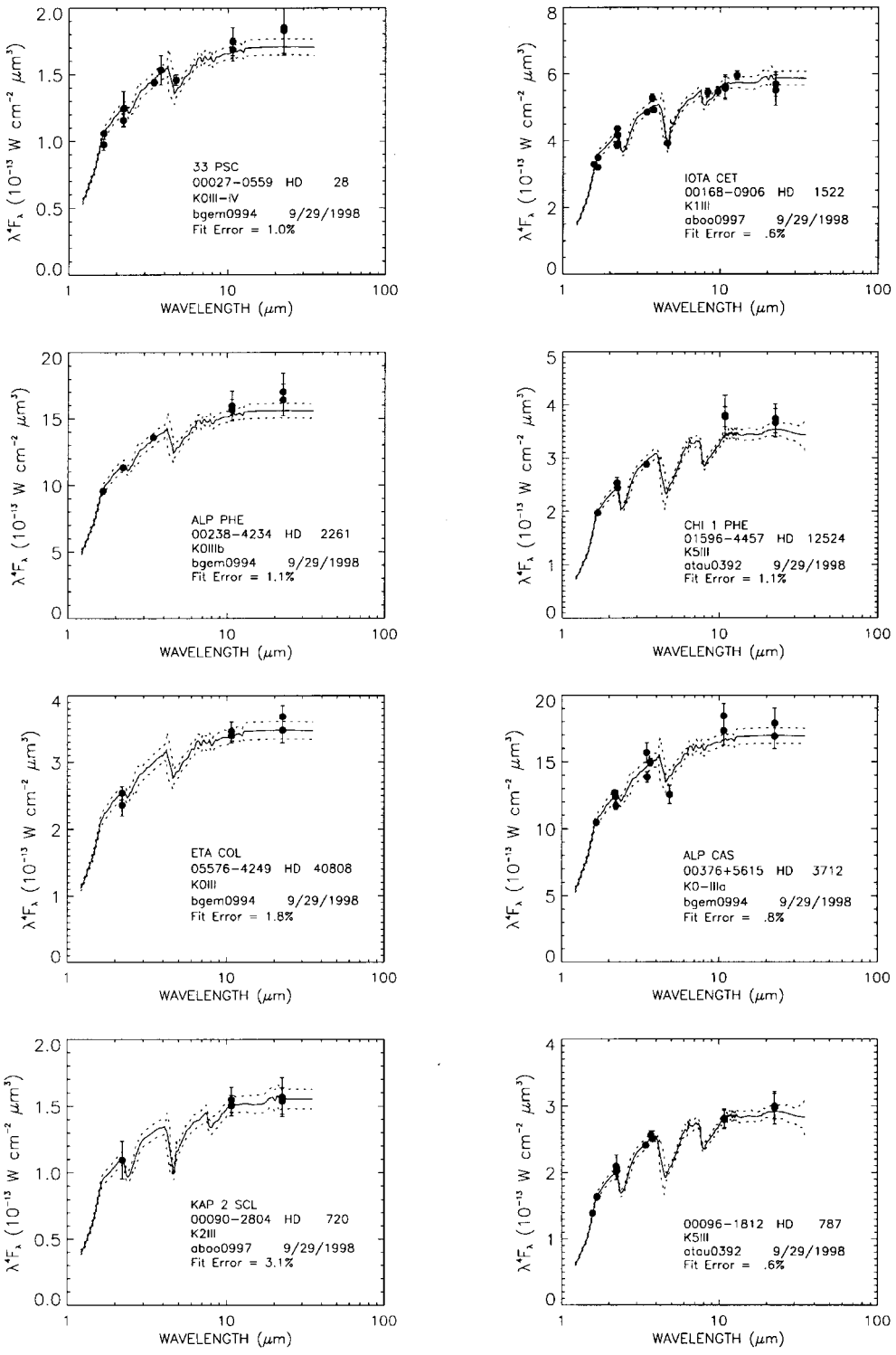

FIG. 3.—Montage of eight representative templates showing the individual characterized photometry used to normalize each template

TABLE 3

ZERO-POINT OFFSETS FOR ALL PHOTOMETRY SYSTEMS WE HAVE CALIBRATED AND USED

Observer	System	Passband	ZPO (mag)	Definition	Citation
D. A. Allen	AAO	BB H	-0.021 ± 0.01	HR 3314 (A0 V)	1
		BB K	-0.012 ± 0.01	HR 3314 (A0 V)	1
		BB L'	-0.029 ± 0.01	HR 3314 (A0 V)	1
A. Alonso	Tenerife	TCS H	0.017 ± 0.010	Vega	2
		TCS K	0.026 ± 0.010	Vega	2
		TCS L'	-0.027 ± 0.011	Vega	2
P. Bouchet	ESO	ESO H	-0.059 ± 0.01	Sirius	3
		ESO K	-0.031 ± 0.01	Sirius	3
		ESO L	-0.012 ± 0.01	Sirius	3
		ESO M	-0.017 ± 0.01	Sirius	3
		ESO H	-0.039 ± 0.009	Sirius	4
		ESO K	-0.014 ± 0.006	Sirius	4
		ESO L	0.014 ± 0.008	Sirius	4
		ESO M	0.007 ± 0.019	Sirius	4
		ESO $N1$	0.111 ± 0.020	Sirius	4
		ESO $N2$	0.014 ± 0.016	Sirius	4
		ESO $N3$	-0.021 ± 0.021	Sirius	4
L. Carrasco	San Pedro Mártir	BB H	0.000 ± 0.003	Vega	5
		BB K	0.000 ± 0.003	Vega	5
B. C.	SAAO	SA H	0.004 ± 0.005	A0 V ensemble	6, 7, 8
		SA K	-0.002 ± 0.005	A0 V ensemble	6, 7, 8
		SA L	-0.002 ± 0.010	A0 V ensemble	6, 7, 8
J. I. Castor	KPNO	OTTO H	0.00 ± 0.01	Vega	9
		OTTO K	0.00 ± 0.01	Vega	9
		OTTO L	0.00 ± 0.01	Vega	9
		OTTO M	0.00 ± 0.01	Vega	9
COBE	DIRBE	Band 2	0.00 ± 0.02	All composites	10
		Band 3	0.00 ± 0.02	All composites	10
		Band 4	0.00 ± 0.02	All composites	10
		Band 5	0.00 ± 0.02	All composites	10
		Band 6	0.00 ± 0.04	All composites	10
D. Engels	ESO	BB H	-0.028 ± 0.02	Sirius	11
		BB K	-0.011 ± 0.02	Sirius	11
		BB L	0.039 ± 0.02	Sirius	11
		BB M	-0.017 ± 0.02	Sirius	11
		BB M	-0.017 ± 0.02	Sirius	12
M. A. Fluks	ESO	ESO H	-0.059 ± 0.01	Sirius	13
		ESO K	-0.031 ± 0.01	Sirius	13
		ESO L	-0.012 ± 0.01	Sirius	13
		ESO M	-0.017 ± 0.01	Sirius	13
J. A. Frogel	KPNO	BB H	0.00 ± 0.01	Vega	14
		BB K	0.00 ± 0.01	Vega	14
G. L. Grasdalen.....	WIRO	BB K	0.02 ± 0.02	Vega	15
		L	0.03 ± 0.02	Vega	15
		M	0.03 ± 0.02	Vega	15
		8.7 μm	0.03 ± 0.02	Vega	15
		10.0 μm	0.03 ± 0.02	Vega	15
		11.4 μm	0.03 ± 0.02	Vega	15
		12.6 μm	0.03 ± 0.02	Vega	15
P. H.	Tenerife	Jn	-0.007 ± 0.010	Vega	16
		Kn	0.000 ± 0.010	Vega	16
		Ln	0.005 ± 0.010	Vega	16
		TCS J	0.001 ± 0.005	Vega	17
		TCS H	0.000 ± 0.005	Vega	17
		TCS K	0.000 ± 0.005	Vega	17
		TCS L'	-0.001 ± 0.007	Vega	17
IRC.....	IRC	BB K	-0.022 ± 0.050	§ 4.3.2	18
IRC/south	IRC	BB K	-0.048 ± 0.050	§ 4.3.2	18
H. L. Johnson	LPL, Tonanzintla	V–BB K	-0.047 ± 0.02	Release 1	19
		V–BB L	-0.025 ± 0.02	Release 1	19
M. F. Kessler.....	IRTF	8.7 μm	0.005 ± 0.008	Composites[a]	20
		9.8 μm	0.014 ± 0.008	Composites[a]	20
		N	-0.010 ± 0.010	Composites[a]	20
		12.5 μm	-0.013 ± 0.010	Composites[a]	20
		Q	-0.003 ± 0.007	Composites[a]	20
M. K.	Tenerife	TCS J	0.001 ± 0.005	Vega	21

TABLE 3—*Continued*

Observer	System	Passband	ZPO (mag)	Definition	Citation
		TCS H	0.000 ± 0.005	Vega	21
		TCS K	0.000 ± 0.005	Vega	21
		TCS L'	-0.001 ± 0.007	Vega	21
J. Koornneef	ESO	BB H	-0.059 ± 0.01	Sirius	22
		BB K	-0.031 ± 0.01	Sirius	22
		BB L	-0.012 ± 0.01	Sirius	22
		BB M	-0.017 ± 0.01	Sirius	22
A. McWilliam	KPNO	2.17 μm	-0.002 ± 0.006	Vega	23
		2.40 μm	-0.007 ± 0.006	Vega	23
		2.17 μm	0.028 ± 0.005	α Leo	23
		2.40 μm	0.046 ± 0.005	α Leo	23
		2.17 μm	0.095 ± 0.009	HR 6092	23
		2.40 μm	0.122 ± 0.009	HR 6092	23
K. N.	Beijing	Xinglong H	0.046 ± 0.020	β Gem, γ Dra	24
		Xinglong K	0.030 ± 0.020	β Gem, γ Dra	24
		Xinglong L	-0.059 ± 0.020	β Gem, γ Dra	24
	Tokyo	ISAS H	0.046 ± 0.020	β Gem, γ Dra	24
		ISAS K	0.030 ± 0.020	β Gem, γ Dra	24
		ISAS L	-0.059 ± 0.020	β Gem, γ Dra	24
M. J. Selby	Tenerife	Kn	0.00 ± 0.01	Vega	25
		Ln	0.00 ± 0.01	Vega	25
M. Tapia	San Pedro Mártir	BB H	-0.04 ± 0.02	Vega	26
		BB K	-0.01 ± 0.02	Vega	26
		BB L'	-0.02 ± 0.02	Vega	26
		BB M	0.01 ± 0.02	Vega	26
A. T. Tokunaga	IRTF	UKIRT N	0.00 ± 0.013	Sirius, Vega	27
		UKIRT Q	0.00 ± 0.013	Sirius, Vega	27
N. S. van der Bliek.....	ESO	ESOKP H	-0.053 ± 0.005	§ 4.3.4	28
		ESOKP H_0	-0.038 ± 0.008	Sirius	28
		ESOKP K	-0.027 ± 0.004	§ 4.3.4	28
		ESOKP K_0	-0.031 ± 0.001	Sirius	28
		ESOKP L'	-0.057 ± 0.004	§ 4.3.4	28
		ESOKP L_0	-0.009 ± 0.010	Sirius	28
		ESOKP M	0.018 ± 0.020	§ 4.3.4	28
		ESOKP N_1	0.034 ± 0.015	Sirius	28
		ESOKP N_2	0.063 ± 0.010	Sirius	28
		ESOKP N_3	0.003 ± 0.017	Sirius	28

[a] The "composites" used to zero-point the "Kessler IRTF" data were α Tau, β Gem, α Boo, and γ Dra.

REFERENCES.—(1) Allen & Cragg 1983; (2) Alonso et al. 1994; (3) Bouchet et al. 1991; (4) Bouchet et al. 1989; (5) Carrasco et al. 1991; (6) Carter 1990; (7) Feast et al. 1990; (8) Table A1; (9) Castor & Simon 1983; (10) Paper IX; (11) Engels et al. 1981; (12) Koornneef 1983b; (13) Fluks et al. 1994; (14) Frogel et al. 1978; (15) Grasdalen et al. 1983; (16) Table A3; (17) Table A2; (18) Neugebauer & Leighton 1969; (19) Johnson et al. 1966; (20) Hammersley et al. 1998; (21) Table A4; (22) Koornneef 1983a; (23) McWilliam & Lambert 1984; (24) Table A5; (25) Selby et al. 1988; (26) Tapia, Neri, & Roth 1986; (27) Tokunaga et al. 1986; (28) van der Bliek et al. 1996.

3.3. *Production of the Final List*

Any star that met all of these criteria was the subject of an additional search of the literature to confirm the nature of the object, its spectral type and luminosity class, and its inclusion in other star catalogs, and to annotate our list with the star's common name. Catalogs and databases searched include the Michigan Spectral Catalogue, Volumes 1 through 4 (Houk, Cowley, & Smith-Moore 1975–1988); the fifth Yale Catalogue of Bright Stars (Hoffleit & Warren 1991); the Catalog of IRC Spectral Types (Bidelman 1980; W. P. Bidelman 1991, private communication); the Infrared Cross-Index (Schmitz, Mead, & Gezari 1987); the Catalog of Infrared Observations (Gezari et al. 1993); and SIMBAD. We deleted from the list all stars newly reclassified with unusual or composite spectral types, or listed as supergiants, or suspected to be variable. Composite types were retained among the binaries and doubles only when the combination of spatial separation and magnitude difference suggested negligible ($<1\%$) contamination of the primary star by its companion.

3.4. *Statistics of the Lists*

Table 1 shows the distribution of those stars finally selected, according to their spectral type and luminosity class. The list is clearly dominated by K and M giants (482 out of the 573); only 87 stars have spectral type earlier than G9.5. This distribution is clearly the result of a compromise between the desire to use stars with relatively uncomplicated spectral energy distributions and the necessity to have them bright enough to be observed in the infrared with at least low-resolution spectrographs.

The spatial distribution of the network of standards is shown in Figure 2. The sky distribution of the current network of self-consistent low-resolution calibrators is shown in Figure 2, which distinguishes the three adopted calibrated Kurucz models (*squares*), the nine observed low-

TABLE 4

STARS FOR WHICH WE HAVE CREATED CALIBRATED TEMPLATES

HD	Spectral Type	Diameter (mas)	Uncertainty (mas)	HD	Spectral Type	Diameter (mas)	Uncertainty (mas)
28.....	K0 III–IV	1.73	0.019	25025.....	M0.5 IIIb	8.74	0.088
720	K2 III	1.73	0.032	25165.....	K5 III	2.05	0.022
787	K5 III	2.52	0.026	25477.....	K5 III	2.01	0.040
1032	M0.5 III	3.07	0.075	25274.....	K2 III	2.02	0.030
1255	M0 III	3.06	0.054	26311.....	K1 II–III	1.78	0.021
1240	M0 III	2.58	0.045	26526.....	M0 III	1.88	0.031
1522	K1 III	3.36	0.036	26846.....	K3 III	1.86	0.019
1635	K3− III	1.81	0.020	26967.....	K2 III	2.76	0.029
1632	K5 III	2.44	0.027	27442.....	K2 IVa	1.95	0.049
1879	M0 III	2.02	0.023	27482.....	K5 III	2.27	0.031
2261	K0 IIIb	5.25	0.060	27639.....	M0 IIIab	3.08	0.039
2436	K5 III	1.99	0.022	27697.....	G9.5 III	2.28	0.024
2486	M0 III	3.45	0.051	28413.....	K4.5 III	1.92	0.050
2637	M0 III	2.38	0.025	28305.....	G9.5 III	2.61	0.035
3346	K6 III	3.24	0.053	28749.....	K3 II–III	2.15	0.040
3712	K0− IIIa	5.47	0.058	29085.....	K0+ III	1.74	0.018
4128	K0 III	5.31	0.055	29503.....	K1.5 IIIb	2.76	0.031
4301	M0 III	2.17	0.024	30080.....	K2 III	1.78	0.035
4502	K1 IIe	2.72	0.036	30338.....	K3 III	2.03	0.052
4815	K5 III	2.19	0.025	31421.....	K2− III	2.74	0.033
5112	M0 III	3.51	0.037	31398.....	K3 II	7.38	0.121
5234	K2 III	1.97	0.021	31767.....	K2-II	2.73	0.044
5462	M0 III	2.36	0.032	31312.....	K5 III	1.88	0.025
6112	M0 III	2.51	0.039	32820.....	K3 III	2.32	0.030
6186	K0 III	1.94	0.031	32887.....	K5 IIIv	6.08	0.064
5848	K2 II–III	2.51	0.065	33554.....	K5 III	2.69	0.030
6805	K2− III	3.44	0.036	33872.....	K5 III	1.93	0.028
6953	K7 III	1.90	0.036	33856.....	K1 III	2.19	0.023
7318	K0 III	1.66	0.029	34334.....	K2.5 III	2.68	0.049
7647	K5 III	2.09	0.035	34450.....	M0.5 III	2.25	0.037
8388	K7 III	2.58	0.048	35536.....	K5 III	2.23	0.027
8498	M0 III	2.52	0.028	36167.....	K5 III	3.66	0.058
8512	K0 IIIb	2.76	0.030	36678.....	M0 III	2.64	0.028
8705	K2.5 IIIb	2.06	0.040	37160.....	K0 IIIb	2.20	0.023
8810	K5 III	2.13	0.065	37984.....	K1 III	1.92	0.021
9138	K3 III	2.58	0.026	38944.....	M0 III	4.24	0.047
9362	K0 IIIb	2.24	0.023	39003.....	K0 III	2.43	0.031
9692	M0 III	1.83	0.021	39523.....	K1 III	2.00	0.052
9927	K3− III	3.69	0.046	39364.....	K0 III	2.63	0.041
10110.....	K5 III	1.91	0.021	39425.....	K1.5 III	3.99	0.047
10380.....	K3 IIIb	2.92	0.030	39400.....	K1.5 IIb	2.46	0.045
10550.....	K3 II–III	2.11	0.037	39853.....	K5 III	2.38	0.027
11353.....	K0 III	2.73	0.029	40091.....	K6 III	2.58	0.042
12524.....	K5 III	2.77	0.032	40035.....	K0− III	2.48	0.026
12929.....	K2− IIIab	6.90	0.074	40808.....	K0 III	2.48	0.034
13520.....	K3.5 III	2.94	0.048	41047.....	K5 III	2.47	0.028
13596.....	M0 III	2.44	0.026	41312.....	K3 III	2.42	0.038
14146.....	M0 III	1.99	0.026	42540.....	K2.5 III	1.95	0.048
14641.....	K5 III	2.20	0.025	42633.....	K3 III	1.82	0.030
14890.....	K2 III	1.91	0.037	43785.....	K0.5 IIIa	1.75	0.025
14872.....	K4.5 III	3.28	0.056	44951.....	K3 III	1.81	0.031
15656.....	K5 III	2.64	0.029	45018.....	K5 III	2.50	0.041
16212.....	M0 III	3.11	0.032	45669.....	K5 III	2.19	0.053
16815.....	K0.5 IIIb	2.18	0.023	46037.....	M0–M1 III	2.20	0.038
17361.....	K1.5 III	1.99	0.030	46184.....	K3 III	1.80	0.027
17709.....	K5.5 III	3.94	0.059	46815.....	K3 III	1.90	0.029
18293.....	K3 III	2.31	0.057	45866.....	K5 III	1.90	0.025
18449.....	K2 III	1.93	0.030	47182.....	K4–K5 III	2.01	0.036
19460.....	M0 III	1.94	0.020	47205.....	K1.5 III–IV	2.44	0.026
19476.....	K0 III	2.28	0.025	47174.....	K2− III	1.97	0.022
19656.....	K1 III	1.94	0.022	47536.....	K2 III	1.74	0.026
20356.....	K5 III	1.87	0.021	47667.....	K2 IIIa	2.63	0.043
20468.....	K2 IIb	2.57	0.035	47914.....	K5 III	2.73	0.029
20644.....	K3 IIIa	3.61	0.045	48217.....	M0 III	2.73	0.043
20893.....	K3 III	1.85	0.029	48433.....	K0.5 III	2.07	0.027
21552.....	K3 III	3.13	0.042	49517.....	K3 III	1.82	0.046
22663.....	K1 III	1.95	0.022	49293.....	K0+ IIIa	1.91	0.023
23249.....	K0+ IV	2.48	0.026	49877.....	K5 III	2.27	0.057
23319.....	K2.5 III	2.12	0.037	49520.....	K3 III	1.96	0.035
23817.....	K2 III	2.80	0.075	50310.....	K1 III	4.49	0.067

TABLE 4—*Continued*

HD	Spectral Type	Diameter (mas)	Uncertainty (mas)	HD	Spectral Type	Diameter (mas)	Uncertainty (mas)
49968.....	K5 III	1.93	0.020	87837	K3.5 IIIb	3.31	0.050
50235.....	K5 III	2.25	0.036	89388	K2.5 II	5.23	0.058
53501.....	K3 III	2.08	0.052	89682	K3 II	3.17	0.035
52960.....	K3 III	2.11	0.036	89998	K1 III	1.72	0.020
52976.....	K6 III	1.96	0.032	90957	K3 III	1.81	0.036
53287.....	M0 III	2.14	0.033	91056	M0 III	4.40	0.112
53510.....	M0 III	2.06	0.021	92305	K5 III	4.86	0.051
54716.....	K3.5 III	2.64	0.039	92682	K3 II	2.19	0.061
55865.....	K0 III	2.50	0.060	92523	K3 III	2.43	0.028
55526.....	K2 III	1.87	0.048	93813	K1.5 IIIb	4.57	0.048
55775.....	K5 III	2.14	0.034	94264	K0+ III–IV	2.57	0.032
57423.....	M0 IIIab	2.94	0.031	94247	K3 III	2.05	0.023
57646.....	K5 III	2.26	0.024	94336	M0 III	1.88	0.025
59311.....	K5 III	2.10	0.034	95212	K5 III	2.16	0.025
59381.....	K5 III	2.26	0.038	95272	K0+ III	2.28	0.026
59294.....	K1 III	2.31	0.027	95314	K5 III	1.92	0.022
59717.....	K5 III	6.86	0.100	95578	M0 III	3.87	0.041
60522.....	M0 III–IIIb	5.00	0.051	96833	K1 III	4.24	0.046
61248.....	K3 III	2.44	0.065	97576	K7 III	2.60	0.049
61338.....	K5 III	3.28	0.038	98118	M0 III	2.99	0.031
61294.....	M0 III	2.52	0.026	98262	K3− III	4.60	0.053
61603.....	K5 III	1.96	0.053	99167	K5 III	3.57	0.038
62689.....	M0 III	1.98	0.056	99998	K3.5 III	3.03	0.034
61935.....	K0 III	2.28	0.023	100029.....	M0 III	6.08	0.067
62044.....	K1 III	2.44	0.029	101666.....	K5 III	2.45	0.028
62285.....	K4.5 III	2.62	0.053	102224.....	K2 III	3.35	0.036
63295.....	K0 III	2.32	0.057	102461.....	K5 III	3.03	0.034
62721.....	K5 III	3.02	0.034	102964.....	K3 III	2.60	0.040
62902.....	K5 III	1.83	0.031	105340.....	K2 II–III	1.87	0.049
63744.....	K0 III	1.67	0.025	105943.....	K5 III	1.91	0.026
63696.....	K5 III	2.16	0.039	106321.....	K3 III	2.20	0.025
63697.....	K3 III	1.88	0.039	107274.....	M0 III	3.34	0.038
64307.....	K3 III	2.02	0.033	107328.....	K0.5 IIIb	1.74	0.018
65662.....	K3.5 II–III	1.97	0.053	108381.....	K1 III	2.15	0.024
65695.....	K2 III	1.90	0.032	108985.....	K5 III	1.79	0.033
66141.....	K2 IIIb	2.68	0.030	109511.....	K2 III	1.66	0.035
67582.....	K3 III	2.39	0.062	109551.....	K2.5 III	2.54	0.039
70272.....	K4.5 III	4.30	0.051	110014.....	K2 III	2.01	0.023
70555.....	K2.5 II–III	2.54	0.037	110458.....	K0 III	1.70	0.018
71701.....	K2 III	2.24	0.057	111067.....	K3 III	2.05	0.022
71095.....	K5 III	2.00	0.022	111335.....	K5 III	2.61	0.034
71093.....	K5 III	1.87	0.019	111862.....	M0 III	1.90	0.021
71878.....	K1 III	2.92	0.073	111915.....	K3.5 III	2.97	0.034
72094.....	K5 III	2.88	0.031	112213.....	M0 III	3.24	0.036
73108.....	K1+ IIIb	2.17	0.023	113092.....	K2 III	1.79	0.026
73471.....	K1 III	2.25	0.034	113996.....	K5− III	3.06	0.032
73603.....	K5 III	2.24	0.025	114326.....	K5 III	1.84	0.021
74442.....	K0 IIIb	2.41	0.031	114780.....	M0 III	2.32	0.026
74860.....	K5 III	2.00	0.023	115046.....	M0 III	2.29	0.026
75691.....	K2.5 III	3.17	0.035	115478.....	K3 III	1.80	0.020
76110.....	M0 III	2.52	0.028	116870.....	M0 IIIv	2.70	0.028
76351.....	K5 III	1.94	0.021	116976.....	K0− IIIb	1.59	0.018
77996.....	K2 II–III	1.85	0.020	119193.....	M0 III	2.09	0.023
77800.....	K5 III	2.67	0.035	120477.....	K5.5 III	4.62	0.050
79354.....	K5 III	2.67	0.030	120933.....	K5 III	5.35	0.059
79554.....	K1 III	1.81	0.020	121710.....	K3 IIIb	2.43	0.026
80493.....	K7 IIIab	7.30	0.078	123123.....	K2− III	3.76	0.040
81146.....	K2 III	2.40	0.036	123139.....	K0− IIIb	5.46	0.058
81420.....	K5 III	2.16	0.023	124547.....	K3− IIIb	2.62	0.039
81799.....	K2.5 III	1.96	0.032	124294.....	K2.5 III	3.31	0.033
82308.....	K4.5 IIIb	4.12	0.046	125560.....	K3 III	1.96	0.021
82381.....	K2.5 IIIb	2.16	0.026	124882.....	K2 III	2.87	0.073
82668.....	K5 III	7.13	0.079	125932.....	K3 III	2.28	0.029
81817.....	K3 IIIa	3.35	0.087	126927.....	K5 III	2.31	0.026
82660.....	K5 III	1.83	0.021	127093.....	M0 III	2.62	0.034
83126.....	M0 III	1.99	0.028	127665.....	K3− III	3.92	0.041
83425.....	K3 III	2.64	0.028	128000.....	K5 III	2.09	0.034
83618.....	K2.5 III	3.50	0.048	128068.....	K3 III	2.08	0.021
83787.....	K6 III	2.34	0.028	128902.....	K2 III	1.99	0.022
85503.....	K2 III	2.93	0.043	129078.....	K3 III	3.96	0.099
86378.....	K5 III	2.18	0.023	130157.....	K5 III	2.10	0.024

TABLE 4—*Continued*

HD	Spectral Type	Diameter (mas)	Uncertainty (mas)	HD	Spectral Type	Diameter (mas)	Uncertainty (mas)
130694.....	K2.5 IIIb	3.22	0.035	181109.....	M0 III	1.97	0.022
132833.....	M0 III	3.15	0.034	182709.....	K4–K5 III	2.32	0.061
133165.....	K0+ IIIb	1.97	0.032	183439.....	M0.5 IIIb	4.40	0.046
133550.....	K5− III	2.07	0.024	184406.....	K3− IIIb	2.30	0.023
133774.....	K5 III	2.84	0.030	184827.....	M0 III	2.84	0.044
135758.....	K0− IIIa	1.91	0.029	184996.....	M0 III	1.97	0.051
136028.....	K5 III	1.87	0.022	186619.....	M0 IIIab	2.27	0.025
136422.....	K5 III	5.69	0.065	186791.....	K3 II	7.06	0.072
137759.....	K2 III	3.73	0.040	187150.....	K5 III	1.94	0.022
137744.....	K4.5 III	2.22	0.025	187660.....	K5 III	1.83	0.020
138265.....	K5 III	1.86	0.022	188056.....	K3 III	1.90	0.020
138481.....	K4.5 IIIb	3.16	0.034	188154.....	K5 III	2.52	0.028
138538.....	K1.5 III	2.56	0.067	188310.....	G9.5 IIIb	1.66	0.021
139669.....	K5− III	2.97	0.035	188114.....	K0 II–III	2.32	0.024
139063.....	K3.5 III	4.27	0.047	188603.....	K2.5 IIb	2.98	0.034
139127.....	K4.5 III	3.39	0.037	189276.....	K4.5 IIIa	3.06	0.032
139663.....	K3− III	2.06	0.021	189319.....	M0− III	6.23	0.064
140573.....	K2 IIIb	4.92	0.053	189140.....	M0 II–III	2.34	0.046
141477.....	M0.5 IIIab	5.49	0.056	189695.....	K5 III	2.01	0.023
141992.....	K4.5 III	3.40	0.041	189831.....	K5 III	2.77	0.029
142574.....	K8 IIIb	2.76	0.029	190056.....	K1 III	2.00	0.023
142676.....	M0–M1 II	1.80	0.047	192107.....	K5 III	2.44	0.030
143107.....	K2 IIIab	2.80	0.030	192781.....	K5 III	1.88	0.021
143435.....	K5 III	2.20	0.024	193002.....	M0–M1 III	2.01	0.053
144204.....	K5 III	1.86	0.020	193579.....	K5 III	1.98	0.027
145892.....	K5 III	2.14	0.023	196171.....	K0 III	3.28	0.034
145897.....	K3 III	2.10	0.023	196321.....	K5 II	3.27	0.037
146051.....	M0.5 III	10.03	0.101	196917.....	M0 III	2.53	0.026
146791.....	G9.5 IIIb	3.00	0.033	197912.....	K0 IIIa	2.10	0.029
149009.....	K5 III	2.37	0.026	197989.....	K0 III	4.58	0.048
149447.....	K6 III	4.68	0.053	198149.....	K0 IV	2.68	0.029
150798.....	K2 II	8.98	0.101	198134.....	K3 III	2.11	0.022
151217.....	K5 III	2.84	0.029	198048.....	K5 III	3.06	0.035
151249.....	K5 III	5.58	0.063	198357.....	K3 II	1.78	0.033
151680.....	K2.5 III	5.99	0.061	198542.....	M0 III	5.16	0.055
152326.....	K0.5 IIIa	1.66	0.027	199101.....	K5 III	2.43	0.026
152880.....	M0–M1 III	2.11	0.035	199345.....	K5 III	2.14	0.024
153210.....	K2 III	3.85	0.041	199697.....	K3.5 III	2.04	0.022
155410.....	K3 III	1.96	0.021	199642.....	K5–M0 III	1.89	0.048
156283.....	K3 II	5.29	0.055	200644.....	K5 III	2.44	0.026
156652.....	M0 III+	1.91	0.024	200914.....	M0.5 III	4.43	0.046
156277.....	K2− III	2.06	0.022	201298.....	K5 III	2.37	0.031
157325.....	M0 III	2.60	0.027	201901.....	K3 III	2.03	0.040
158996.....	K5 III	1.92	0.024	203399.....	K5 III	1.95	0.032
157999.....	K2 II	3.24	0.035	203504.....	K1 III	2.42	0.030
158899.....	K3.5 III	3.06	0.032	205478.....	K0 III	2.42	0.064
161096.....	K2 III	4.63	0.049	206445.....	K2 III	1.81	0.020
163588.....	K2 III	3.13	0.033	209688.....	K3 III	2.71	0.030
163376.....	M0 III	4.13	0.042	211416.....	K3 III	5.99	0.064
163770.....	K1 IIa	3.15	0.034	213310.....	M0 II + B8 V	5.43	0.069
164646.....	M0 IIIab	2.42	0.027	214868.....	K2.5 III	2.69	0.029
168323.....	K5 III	2.21	0.031	216032.....	M0 III	5.12	0.053
168775.....	K2− IIIab	2.28	0.025	216446.....	K3 III	2.28	0.059
168723.....	K0 III–IV	2.98	0.032	216149.....	M0 III	2.07	0.021
168592.....	K4–K5 III	2.66	0.047	216397.....	M0 III	3.38	0.035
169414.....	K2 IIIab	3.03	0.032	217902.....	K5 III	2.37	0.027
169916.....	K1 IIIb	4.24	0.047	218452.....	K5 III	2.14	0.024
170693.....	K1.5 III	2.03	0.029	218670.....	K1 III	2.34	0.027
170951.....	M0 III	1.76	0.023	219449.....	K1− III	2.24	0.025
171759.....	K0 III	2.63	0.065	219784.....	K1 III	2.13	0.025
173780.....	K2 III	1.95	0.021	219981.....	M0 III	2.01	0.021
174387.....	M0 III	2.89	0.032	220009.....	K2 III	1.99	0.022
175775.....	K1 III	3.37	0.036	220088.....	M0 III	2.35	0.025
176524.....	K0 III	1.69	0.023	220363.....	K3 III	1.99	0.022
176670.....	K2.5 III	2.41	0.026	220440.....	M0 III	2.38	0.026
177808.....	M0 III	2.40	0.026	220954.....	K0.5 III	2.00	0.021
177716.....	K1.5 IIIb	3.93	0.043	221588.....	M0 III	2.48	0.046
178345.....	K0 II	2.42	0.025	222404.....	K1 III–IV	3.38	0.052
179886.....	K3 III	1.95	0.033	224630.....	K5 III	2.49	0.028
180450.....	M0 III	2.87	0.032	224889.....	K3 III	2.29	0.061

NOTE.—Table 4 appears in expanded form in the electronic edition of the Astronomical Journal.

resolution composites (*circles*), and the 422 calibrated templates (*crosses*). The calibrators are well distributed over the sky with the exception of several notable regions where the star density is low or zero. These are a region within about 15° of the Galactic center, a 10° diameter region centered on the Large Magellanic Cloud, two regions near the north Galactic pole, and the *IRAS* 50° unsurveyed gap. There are another 123 stars that meet all our selection criteria but lack a luminosity classification. These stars are all north of declination −20°, testifying to the need to extend the Michigan classification project to the northern sky. The brightest star (α Boo) has 793 Jy at 12 μm. There are 14 stars brighter than 100 Jy at 12 μm, and 246 stars brighter than 10 Jy at 12 μm. The faintest stars have 5 Jy at 12 μm, giving us over 2 orders of magnitude in mid-infrared dynamic range in the network.

4. NEWLY CHARACTERIZED FILTER SYSTEMS

4.1. *Absolute Calibrations for Zero Magnitude*

Table 2 indicates those systems and filters for which we have been able to secure full, cold, passband details and whose photometry we have been able to use in template normalization. We calculated terrestrial transmission curves specific to all the relevant observing sites, altitudes, and dates of observation using the PLEXUS (Clark 1996) code and included a generic InSb radiance response curve when applicable. (Note that some authors, such as Alonso, Arribas, & Martínez-Roger 1994, already incorporate their detector's response in their published filter profiles, for example, for the broad passbands of the Tenerife 1.5 m reflector [hereafter TCS = "Telescopio Carlos Sanchez"].) The product of these three components for filter, atmosphere (when appropriate), and detector constitute our archived "system response curves." For every such curve, Table 2 presents our absolute calibrations in the form of the in-band irradiance for zero magnitude, its absolute uncertainty, the bandwidth, the associated isophotal flux density F_λ, and isophotal wavelength. These attributes were determined by integrating each system response curve over our calibrated Vega spectrum (Paper I), which we take as our definition of "zero magnitude" at all infrared wavelengths. When we lacked the actual uncertainties in the measurement of a filter's transmission curve, we assigned a wavelength-independent fractional uncertainty of 5%. This component of error is in addition to the absolute uncertainty ("global bias"; see Paper I) associated with the Vega spectrum (1.45%). Together, these components provide the

TABLE 5

INFORMATION ACCOMPANYING A CALIBRATED TEMPLATE

```
IRAS PSC Name:  11147+0217
IRAS FSC Name:  F11147+0217
75 LEO          HR 4371     HD 98118    M0III
IRC             203

Release 2.1
Date and time template processed:  9/29/1998 14: 4
Composite Spectrum Used: band1093.tem
Av(composite) = .00 Av(star) = .00
Stellar Diameter (mas) = 2.99 +/- .031

================================================================
Photometry Used For Template Normalization:

 Reference          Band          Mag           dMag          Iso_Wav       Iso_Flux      Flux_Unc
 FLUKS 1994         H             1.599         .017          1.676         .279E-13      .565E-15
 FLUKS 1994         K             1.400         .017          2.216         .114E-13      .226E-15
 FLUKS 1994         L             1.253         .009          3.790         .164E-14      .248E-16
 FLUKS 1994         M             1.534         .034          4.711         .539E-15      .189E-16
 JOHNSON 1966       V-K           3.760         .030          2.231         .112E-13      .449E-15
 MCWILLIAM 1984     2.17          1.328         .015          2.170         .123E-13      .213E-15
 MCWILLIAM 1984     2.40          1.546         .015          2.406         .685E-14      .123E-15
 NOGUCHI_T 1994     H             1.490         .030          1.674         .282E-13      .933E-15
 NOGUCHI_T 1994     K             1.320         .030          2.220         .115E-13      .383E-15
 IRAS FSC           12            12.890        .773          10.850        .281E-16      .170E-17
 IRAS FSC           25            3.191         .255          22.530        .156E-17      .129E-18
 IRAS PSC           12            12.800        .640          10.850        .278E-16      .140E-17
 IRAS PSC           25            3.260         .293          22.530        .157E-17      .146E-18
 IRC                K             1.398         .040          2.231         .111E-13      .632E-15

Notes:
1.  IRAS PSC and FSC Mag and dMag are in Janskys.
2.  Iso_Wav is the isophotal wavelength in microns (um).
3.  Iso_Flux and Flux_Unc are the flux and flux uncertainty 1 (sigma)
at the isophotal wavelength in Watt/cm2/um.
4.  Johnson colors (e.g., V-K) are archived. Thus MAG and dMag
refer to a color index, but Iso_Wav, Iso_Flux, and Flux_Unc
refer to the non-V filter.
```

error in the calculated in-band flux. The error associated with the isophotal flux density is strictly somewhat larger than that in the in-band irradiance because F_λ is derived from the in-band flux by dividing by the bandwidth, which has formal uncertainties of its own.

The narrow bands of Selby et al. (1988) are of particular value because their passbands sample the cleanest parts of the terrestrial transmission. One of us (P. H.) has continued to make measurements with these filters. Any systematic differences between P. H.'s magnitudes and those of Selby et al. for stars in common are within the noise.

4.2. *Zero-Point Offsets*

We also require the basis star(s) of any set of measurements. For many northern observers, Vega fills this niche. Consequently, if an observer publishes system magnitudes for Vega and these are not all zero, we can readily bring these magnitudes into our own context by forcing Vega to be zero. The algebraic quantities needed to achieve this are the "zero-point offsets" (ZPOs). Not every set of measurements includes Vega. Sirius can equally well provide us with the system offsets once we have calibrated it with respect to the zero magnitudes for the relevant system. Likewise, we can define the offsets if a set of measurements includes any cool giant stars for which we have created composite spectra.

Table 3 presents all the ZPOs for photometry data sets used to create templates. Note that a single system, such as the traditional ESO near-infrared filters, can have several sets of observers, each of whose measurements may be subject to different ZPOs. The fifth column of Table 3 indicates observations of exactly which star(s) were used to define any ZPO for each observer. The final column in this table gives a citation to the publication in which the relevant photometry appears.

Each of Tables A2, A3, and A4 is organized so that measurements of Vega appear at the top, followed by data on any stars for which we have assembled and published a composite spectrum and, finally, data for typical stars of the network. Table A1 (B. C.'s SAAO measurements) has as basis an ensemble of B and A dwarfs. Vega itself is not observable from South Africa, and the signal-to-noise ratio obtained on the very bright Sirius does not reflect the real uncertainties in the system basis. The SAAO system, and its self-consistency, is described in detail by Carter (1990, 1993) and by Glass (1985, 1993), who also provide the relevant transformations between SAAO and the CTIO system, the zero-magnitude basis of which is Vega. Table A5 (K. N.'s work) was zero-pointed at HKL through his observations of β Gem and γ Dra. We cannot define an accurate zero point for J because our basis stars are these two K giant composites. Further, after careful cross-checks between K. N.'s work and other characterized photometry from much higher sites, we decided not to use his L-band data for template scaling. This conservative approach is in keeping with the very low elevations of the Tokyo (sea level) and Xinglong (800 m) sites.

4.3. *Testing the New Photometry for "Closure"*

We would like to ensure that our well-characterized systems demonstrate "closure," in that their magnitudes for all our composites yield exactly what we would expect when integrating their passbands over these cool stellar spectra. To exemplify this closure we offer tests of P. H.'s photometry. First we treat his narrowband photometry in the Selby et al. (1988) bandpasses. The data set in Table A3 includes stars newly measured by P. H. but without observations by Selby et al., and remeasurements to greater precision by P. H. that were selected from Selby's archive. Table A3 incorporates data on all our composites, so we have integrated combined filter, detector, and atmosphere profiles over the composites to define our expected magnitudes. We have examined the ensemble average of differences in the sense of Table A3 minus expectation for those bands we are able to integrate over our composite spectra. These yielded Kn, 0.004 ± 0.003; Ln, -0.007 ± 0.005. After applying the zero-point offsets (from Table 3), we found the final differences to be 0.004 ± 0.003 and -0.002 ± 0.005 for the two relevant passbands. Kn and Ln are clearly consistent with zero, indicating a self-consistent set of magnitudes.

We have applied the identical analysis to P. H.'s broadband data (Table A2) using Sirius and the seven cool composites. These yielded ensemble mean "observed minus expected" values of H, -0.019 ± 0.015; K, $+0.002 \pm 0.013$. After zero-point corrections (Table 3), we found final mean differences of -0.019 ± 0.015 and $+0.003 \pm 0.013$ for the HK, respectively. Again, H and K are clearly consistent with zero. So we likewise conclude that P. H.'s broadband measurements are self-consistent in the mean.

Both the Jn and J filters cut on slightly before our composites' starting wavelengths, so we cannot use these photometry points to scale any templates in the present paper. This implies that the magnitudes created from our set of composite spectra and presented in Table 3a of Paper IV for both Jn and J should be treated strictly as approximations. All Jn and J are potentially too faint by about 0.02 mag. This effect does not affect any of the other magnitudes in Paper IV, because all the other passbands are entirely contained within our 1.2–35 μm range, and in no way influences the scaling of templates because, again, Jn and J are never used for this purpose.

4.3.1. *Other Useful Photometry Archives*

Table 2 summarizes all sets of photometry data that we have been able to utilize. The most abundant contributors (ranked in descending order of data directly useful to us for template scaling) have been *IRAS*, "IRC" (§ 4.3.2), B. C. (Table A1), the "ISO Ground-Based Preparatory Programme" (hereafter GBPP; § 4.3.4), Tenerife broadband programs (Tables A2 and A4), Johnson, the older ESO archives (J. Koornneef; P. Bouchet and colleagues), and K. N. (Table A5). Of course, both *IRAS* and IRC measurements suffer from appreciable formal uncertainties, so that these data carry less weight in determining the mean scale factor of a template than do precision near-infrared (ground-based) data.

Some noteworthy aspects of our usage of photometry, not presented for the first time in this paper, appear below.

4.3.2. *The Caltech Two-Micron Sky Survey*

For many of our K and M giants, the Caltech Two-Micron Sky Survey (Neugebauer & Leighton 1969, hereafter IRC) provides K-band magnitudes, albeit measured with a PbS cell. An archival search at Caltech failed to produce a profile of the transmission of the actual K filter, so we adopted Bessell & Brett's (1988) overall system response curve. In addition to the published IRC, we were

able to utilize the unpublished southern extension (to declination $-42°$), thereby adding another 700-plus stars to our IRC archive. Because of the rather large magnitude uncertainties in both the IRC data sets (typically 0.06 mag), we felt it important to assess the actual zero-point offset and its uncertainty from a large body of stars. Consequently, we created the new generation of calibrated templates first without using any IRC data. Then we integrated all these new templates over the IRC passband and compared our synthesized IRC K magnitudes with those of the IRC and IRC/south separately. This provided us with separate zero-point corrections for the IRC and IRC/south (see Table 3). The photometric uncertainties of the IRC/south were magnitude dependent; thus we adopted a 0.05 mag error for $K < 2.0$ and 0.06 mag for $K > 2.0$, derived from the median uncertainty in each 1 mag bin.

4.3.3. *IRAS*

For every star in the network, we have *IRAS* 12 and 25 μm data from both the PSC and the Faint Source Survey/Catalog (Moshir et al. 1992, hereafter FSC). We translated both the PSC and FSC flux densities into our context (cf. Paper I) by multiplying by appropriate factors. For the PSC we used 0.976 ± 0.007 and 0.936 ± 0.022 at 12 and 25 μm, respectively (Table 3 of Paper I). To create the corresponding factors for the FSC we simply compared the ratio of FSC to PSC flux densities for 525 stars from the Walker-Cohen atlas with spectral types late G to early M III. This gave $\mathrm{FSC12/PSC12} = 0.994 \pm 0.003$ and $\mathrm{FSC25/PSC25} = 0.989 \pm 0.003$. We made use of both PSC and FSC flux densities because they represent independent methods of analyzing the original *IRAS* data. In 1994 October we analyzed the distribution of scale factors implied by *IRAS* data from the first set of templates to determine what *IRAS* alone would have given, in the absence of any supporting ground-based photometry. The distribution was symmetric about 1, with a standard deviation of 0.041. Therefore, we concluded that any star having only *IRAS* photometry is subject to an additional source of uncertainty of 4.1%, which is included in the error budget in the new set of templates for such sources.

4.3.4. "*ISO Ground-Based Preparatory Programme: An ESO Key Programme*"

In support of *ISO*, ESO organized a major ground-based photometry program of several hundred stars across the southern sky (van der Bliek, Manfroid, & Bouchet 1996), with extension to the north by P. H. The basic effort was directed toward securing near-infrared data in the common passbands of *JHKL*. The southern work also obtained data in five near-infrared narrow bands on many stars, supplemented occasionally by measurements in two broad and three narrow bands in the 10 and 20 μm regions. We used data from the three near-infrared narrow continuum filters (H_0, K_0, L_0) and from all but the broad 10 μm band among the bolometer observations. There was also a brief mid-infrared foray into the north, using the Infrared Telescope Facility (IRTF), that took measurements of about 20 K and M giants in three narrow bands near 10 μm and at 20 μm. These latter observations took place in February/March of 1992, were analyzed with a multinight reduction technique by P. H. and delivered to *ISO* Calibration Liaison in 1995 November (hence their reference as IRTF_ISO 1995 in template headers), and have appeared as Hammersley et al. (1998). All the relevant ESO passbands were recharacterized and archived at VILSPA with the photometry, in support of *ISO*. For those from the IRTF, we had already obtained copies of the original manufacturer's filter transmission curves.

The original criteria for star selection by ESO were very different from those of our own network and resulted dominantly in warm dwarfs. However, a number of stars are in common with the Walker-Cohen network, particularly among the infrared-brighter stars covered at the longer wavelengths. The southern data furnish valuable photometry for an appreciable number of stars in our network. The near-infrared narrowband ESO measurements included Sirius, which provided direct information on the system's zero points. The *JHKLM* data set encountered problems with the brightness of Sirius and consequent nonlinearities in the electronics, so we preferred to determine the zero points at *HKLM* by an alternative, more robust, method. We first created templates using all photometry sets available to us with the sole exception of these ESO Key Programme *HKLM* data. For the 29 stars that have these ESO *HKLM* observations, we synthesized the broadband magnitudes by integrating each of the four passbands over the complete templates. The average difference for each of the four filters between the synthesized and the observed Key Programme magnitudes defined the requisite zero points.

4.3.5. *Other Useful Characterized Photometry*

In addition to the aforementioned photometry in characterized passbands, we located two other data sets that we were able to characterize adequately to the point where they provide valuable data to constrain the scaling of templates. The first is DIRBE, with flux densities drawn from the special subset of DIRBE's own calibrators (Hauser et al. 1997). Zero-point offsets were established as essentially zero by Cohen (1998), and his associated zero-point uncertainties were used (Table 3).

The second is from McWilliam & Lambert (1984), who give filter profiles for two narrow bands near 2.17 and 2.40 μm, to which we added our mean atmospheric transmission curve for Kitt Peak and the detector's spectral response function. The resulting system passbands were archived and integrated over our calibrated model for Vega (Paper I) to provide "zero magnitude" values of the in-band fluxes and isophotal flux densities (Table 2). McWilliam & Lambert (1984) observed over 100 late K and M giants through these two filters and in a broad J band, setting their color indexes by Vega, which should have resulted in adequate zero points. However, two other "standard stars" were used for sky coverage. A. McWilliam (1996, private communication) has kindly provided us with full details so we know which of the three reference stars (Vega, α Leo, HR 6092) was used for each published program giant. From his detailed notes one can see that the J magnitudes adopted for the other two standards were discordant with the zero point for Vega by about 0.08 mag (α Leo) and 0.06 mag (HR 6092). These offsets in no way affect the measurements, or the conclusions, of McWilliam & Lambert (1984), who treated their stars solely in terms of color indexes, adjusted to zero index for Vega. But, for our purposes, it is clearly essential to define separate zero-point offsets for each cool giant, based on the actual standard star used.

A total of 34 McWilliam-Lambert program stars are in common with the set of 183 (first generation) templates that we created in 1994 October to test and establish the tech-

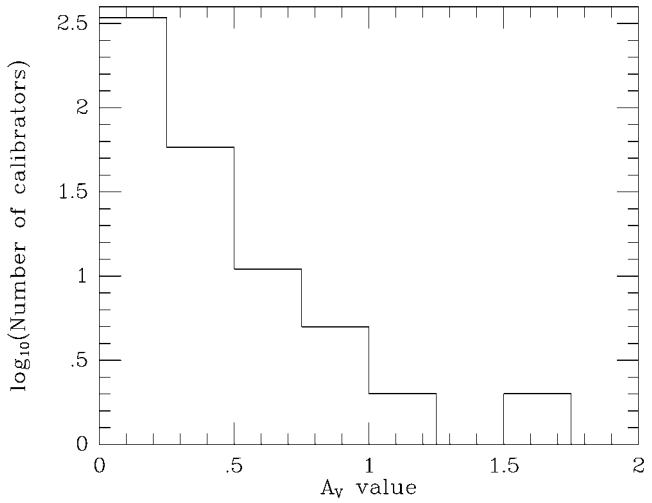

FIG. 4.—Distribution of extinction values toward the 422 K/M giants

niques described in the present paper. One star with a published absolute spectrum, γ Dra, was also measured. We integrated these two system passbands over the 34 calibrated templates and one composite spectrum to define our expected values for [2.17] and [2.40], along with formal uncertainties based on both the original composites and on the bias (§ 6) additionally associated with each of the individual calibrated templates.

These 35 stars fall into three groups: 13 stars were referred directly to Vega, 17 to α Leo, and five to HR 6092. We assigned individual errors to the McWilliam-Lambert observations using the typical uncertainties they specify, with slight reductions for stars measured more than once. Direct comparisons of our expected magnitudes with those observed by McWilliam & Lambert yielded the zero-point offsets for this data set (Table 3). Our tabulated measurement errors also accommodate (in quadrature with the photometric measurement errors) the uncertainties with which we have been able to define these three pairs of zero-point corrections. Once we defined the three sets of zero-point offsets from the first-generation templates for these 35 fiduciary stars, we were able to use McWilliam & Lambert photometry as part of the process for making new templates for these stars, and for 11 other stars in our network.

5. THE TEMPLATE CODE

The creation of a calibrated spectral template for a star begins with selection of the star from the input list of stars to be templated. The input list is organized by *IRAS* name and also contains other designations for the star, such as the HD, HR, and IRC numbers; a star's common name; a spectral type and luminosity class; V, $B-V$, $U-V$; and the *IRAS* PSC and FSC 12 and 25 μm photometry. A smoothed composite is then selected that matches the spectral type and luminosity class of the star and is corrected for extinction (see § 2) along the line of sight to the star. Our photometry database is then searched for observations of the star. The photometry database is indexed by *IRAS* name and contains for each observation of the star the observed magnitude and its uncertainty, the name of the filter used, and a reference to the observer. These data are essential to recovering the proper relative system spectral response curve (filter), zero-point offset (see Table 3), and zero-magnitude flux calibration (see Table 2). A filter is selected. The observed magnitude in that filter is corrected for zero-point offset and then converted to an observed in-band flux using the zero-magnitude flux calibration. Next the spectral irradiance of the extinction-corrected, smoothed composite is integrated over the spectral passband corresponding to the observed magnitude, producing an in-band flux for the composite. The ratio of the observed in-band flux to the composite in-band flux and its variance are then calculated. This process is repeated for each photometric measurement of the star. The inverse-variance–weighted mean ratio is then determined and the new calibrated spectral template produced as the product of the mean ratio times the spectral irradiance of the extinction-corrected, smoothed composite. The errors of the new template are calculated from those of the original composite with the global bias component combined (root sum squared) with the error in the mean ratio (see Paper IV for a discussion of global and local biases).

We took stellar spectral classifications from a variety of sources, favoring the Perkins revised types of Keenan & McNeil (1989) when available, or the Michigan Spectral Catalogue, or the fifth version of the Yale Catalogue of Bright Stars (ranked in order of preference). These were applied over a range of ± 0.5 of a spectral subclass, so, for example, we applied the template derived from β Gem (K0 IIIb) to any star between G9.5 III and K0.5 III. On the basis of analysis of the small differences between our composites for α Tau (K5+ III) and β And (M0+ IIIa), we additionally applied the K5 template to stars with types K5–M0, K6, K7, and K8 III.

None of the stars for which we have already published low-resolution composite spectra were retained in the set of objects to be templated. Thus, α Tra, a K3 III for which Paper VI presents only a 3–35 μm high-resolution spectrum, is templated at low resolution in the present paper based on the 1.2–35 μm K3 III spectrum of Paper IV.

We did not use Koornneef's (1983a) homogenized photometry when photometry from Bouchet, Manfroid, & Schmider (1991) was available, because these latter authors rereduced all the ESO data together, thereby subsuming Koornneef's work. We also found, after detailed comparisons between Table A5 and other L-band data on stars in common, that our own 3.5 μm measurements from low-altitude sites in China and Japan have rather large uncertainties compared with those in JHK, and we preferred not to use any of these L-band data.

Figure 3 presents a montage of eight calibrated stellar templates, offering a variety of different spectral types and available sets of photometry. The templates are shown in λ^4-F_λ space, highlighting the essentially Rayleigh-Jeans character of the long-wavelength continua.

6. STATISTICS OF THE TEMPLATES CREATED

Several distributions are of interest, namely, those for the extinction values that we applied to the templates, the number of characterized photometry points available to normalize each template, the template biases, and the derived angular diameters.

Only 83 of the 422 calibrators were determined to have nonzero extinction, and the distribution by A_V appears in Figure 4. At our current limiting flux density, most of these cool giants are within the Local Bubble.

The frequency of photometric observations (Fig. 5) clearly indicates the members of the network for which

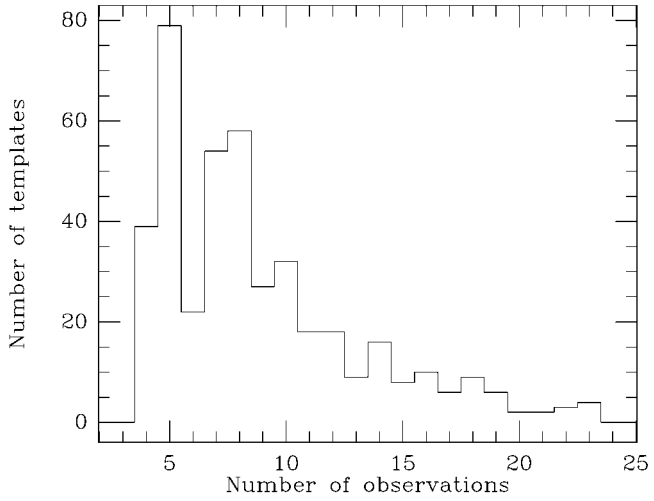

FIG. 5.—Distribution of the number of available photometry points used to normalize each of the 422 calibrated spectral templates.

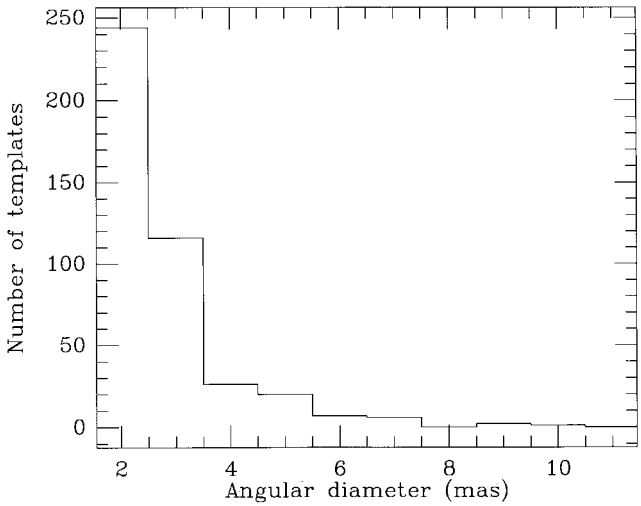

FIG. 7.—Distribution of our derived angular diameters

IRAS data alone provide the template normalization. These stars have only four photometric (PSC and FSC) measurements. Typical network calibrators have five to 10 measurements available for template scaling, reducing the resultant template bias by about a factor of 3 over that for an object with only *IRAS* data. Stars with 11–23 measurements have biases reduced by a further factor of 2.

Figure 6 shows some evidence for a trimodal distribution in template biases. Stars in the sharper peak centered at about 1% represent 64% of the total. The 26% of the sample in the peak with bias centered at $\sim$2.75% are stars for which we would like to secure more precise photometry in order to move them into the major peak associated with stars with the best available data. The peak centered at 4.75% arises from objects that entirely lack precision near-infrared photometry and were templated on the sole basis of their *IRAS* flux densities (perhaps augmented by an IRC or Johnson *K* magnitude).

Figure 7 illustrates the histogram of angular diameters for the new calibrators. This is sharply peaked, as expected from consideration of source counts, in the smallest bin between 1.5 and 2.5 mas. Diameters of this order have been measured by van Belle et al. (1999), using the Palomar Testbed Interferometer for visual intensity measurements in the *K* band. In Figure 8, we compare directly observed diameters from a variety of sources with our own, labeled "radiometric diameters." The vast majority of the observed diameters were derived by interferometric techniques (Di Benedetto & Rabbia 1987; Mozurkewich et al. 1991; Quirrenbach et al. 1996; Di Benedetto 1993; Dyck et al. 1996; Dyck, van Belle, & Thompson 1998; van Belle et al. 1999), either at optical (0.45–0.80 μm) wavelengths or in the *K* band, but lunar occultations (e.g., Ridgway et al. 1982) also provide valuable measurements. Our reference radiometric diameters were derived from the bright composites by fitting stellar model spectra that incorporate the effects of limb darkening, so our diameters are purely geometric, that is, they represent "true diameters." This comparison with the literature was, therefore, made in terms of true diameters, adopting the various authors' conversions from uniform-disk diameters to limb-darkened diameters based on Manduca, Bell, & Gustafsson (1977) and Manduca (1979). This conversion process is not without some uncer-

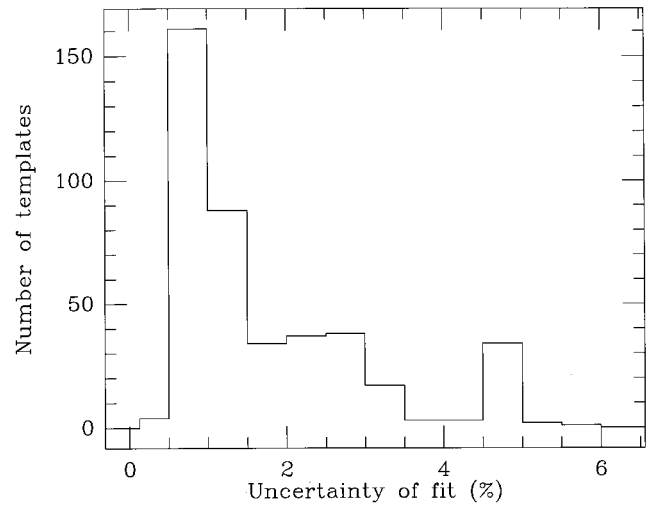

FIG. 6.—Distribution of template biases among the 422 templates

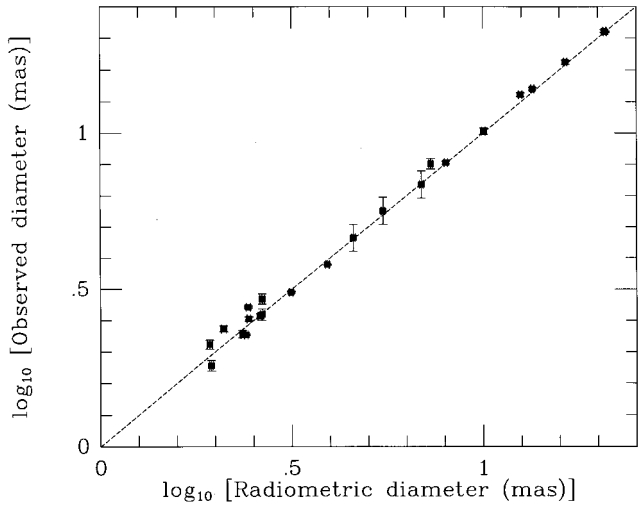

FIG. 8.—Comparison of stellar angular diameters observed either interferometrically or during lunar occultations with those we derive radiometrically. The dashed line passes through the origin with slope 1 and is intended to guide the eye.

tainty, but even the total correction at 0.45 μm from uniform-disk to true diameter amounts to only a few percent, and the conversion at K is only 2.2% (van Belle et al. 1999). The agreement between radiometric and observed diameters is highly satisfactory: the formal least-squares best-fitting relation between (linear) diameters gives (observed) = (1.013 $\pm$ 0.008)(radiometric) + (0.035 $\pm$ 0.073). Thus our method leads to sensible diameters with formal errors significantly smaller than those associated with visual intensity measurements on stars at this brightness level ($K \leq 3.0$), even in the 1–2 mas range.

Table 4 summarizes the 422 stars for which we have created templates. For brevity, the version of this table that appears in the printed paper lists just HD numbers (because these designate the file names of the calibrated spectral templates) and the derived angular diameters (with their uncertainties) in milliarcseconds. The electronic version contains much more complete information on each star and presents *IRAS* designations, common names, HR and HD numbers, the extinctions we applied to the templates, the angular diameters with uncertainties, the template biases, and the number of photometry points used to normalize each individual template. To preserve the relationship between these two versions, note that Table 4 is ordered by implicit *IRAS* name or, effectively, by B1950.0 right ascension.

7. TEMPLATE FILES AND HOW TO OBTAIN THEM

A detailed header precedes every template created in this manner. This header is accompanied by various names for each star (its *IRAS* name, common name, HR and HD numbers); release version, date, and time of template creation; the template spectrum used; the extinctions of both the bright star that gave rise to the template shape and of the templated star; the angular diameter deduced for the stellar template (derived from the template scale factor and our published values of angular diameters for the bright composite spectra, in Paper VII); every piece of characterized photometry used to normalize the template, with abbreviated references; full citations of the publication of this photometry; and our determinations of isophotal wavelength, isophotal flux, and its uncertainty. Using these tabulations, a user can construct plots identical to those shown in Figure 3.

The current release version is 2.1 (release 2.0 represented a "beta" version). Table 5 illustrates the header for HD 98118. Templates are always named for their HD designations; hence "HD98118.tem" will represent the file associated with this star.

The actual calibrated stellar spectra have a five-column format (as do the models and composites described in Papers IV–VII). We tabulate wavelength (μm), monochromatic irradiance (F_λ in units of W cm^{-2} μm^{-1}), total uncertainty (also in units of W cm^{-2} μm^{-1}) associated with this value of F_λ, local bias, and global bias. For most applications, "total uncertainty" is the error term most appropriate to use. It is the standard deviation of the spectral irradiance and incorporates the local and global biases. Local and global biases are given as percentages of the irradiance. The global bias does not contribute error to flux ratios or color measurements, and may be removed (in the root sum square sense) from the total error. Note that we prefer to provide pristine data, rather than to regrid each composite or template to an equally spaced or common wavelength scale. Each composite has a different set of wavelengths. Consequently, template spectra are *not* tabulated at equal intervals of the wavelength but, rather, at the wavelengths of the originally observed composite spectra.

Our models and composites are available through the AAS CD-ROM series, Volumes 5 and 7 (Papers IV, VI, and VII), with the exception of the spectrum of α Tau, which has been included in the electronic version of the present paper. All the templates described herein likewise appear in the electronic edition of the Astronomical Journal.

8. CONCLUSIONS

We have developed a self-consistent, all-sky, network of over 430 infrared radiometric calibrators within a carefully constrained absolute framework following our definitions of "zero magnitude" for characterized photometric systems. Currently this network includes three types of calibrator: models, composites, and templates. *Models* connotes the three calibrated Kurucz models for Sirius, Vega (Paper I), and α^1 Cen (Paper VI). *Composites* refers to the IR-bright K and M giants (and these are generally the brightest stars in the current network) as described in Papers II and IV–VII. *Templates* form the substance of the present paper, represent the bulk of the network, and extend to irradiance levels about 150 times below that of the brightest composites.

The self-consistency arises because of the rigorous framework in which we have united both photometry and spectroscopy, and have constructed composites from their ratios to the modeled stars, primarily Sirius. Further, it has been possible to validate the self-consistency of the fainter members of this network through the Near-Infrared Spectrometer (NIRS; Noda et al. 1994), a 1.4–4.0 μm, low-resolution ($\approx$0.11 μm), grating spectrometer carried aboard *IRTS*. No *IRTS* scan passed over any of the model or composite stars. Therefore, the calibration was established through the use of calibrated templates. A set of four absolute calibrators was chosen (IRC +50276, θ Cnc, θ Her, and κ Gru). Using any of these calibrators to establish the conversion between raw signals and physical units, the resulting agreement between the observed spectra of the others and their independent, and unused, templates is remarkably good (cf. Matsumoto & Murakami 1996), $\leq$2%. The templates for these four stars are based on three different composites (K1.5, K5, and M0 III) and represent irradiance levels between 30 and 80 times fainter than their respective composites. This represents the first step in validating our fainter products and in demonstrating the self-consistency of the current network.

Such a network is entirely possible within an absolute radiometric tolerance of 5% between 1.2 and about 15 μm, and about 10% from 15 to 35 μm, figures of merit in keeping with external demands imposed on satellite programs. We advocate use of this network to support a wide range of astronomical observations, be they ground-based, airborne, or satellite sensors, because of the ongoing need to pursue a unified approach to infrared calibration *with a traceable pedigree*. Such a network of complete spectra is highly flexible and makes no assumptions whatsoever about any future filter profiles. It avoids the need for complex magnitude and color transformations between new and old photometric systems, at least as far as the assignment of in-band, or specific monochromatic, absolute flux densities at isophotal wavelengths or frequencies are con-

cerned. The network is capable of the accurate definition of real characteristics of new systems with arbitrary passbands, including nonstandard passbands like the short K' of the DENIS and 2MASS projects, response curves notched to avoid deep terrestrial absorptions, and complex or divided bandpasses, such as result through the use of near-infrared "OH suppressing" filters.

To enhance the quality of the current network would require new precision ground- or space-based photometry of stars with the spectral types for which we now have complete low-resolution templates. Such data would both carry more weight in the normalization of a template than older photometry with larger uncertainties (because of our inverse-variance weighting scheme for template multipliers) and perhaps provide near-infrared "anchor" points for stars templated with *IRAS* data alone. We might also seek to make templates more specific to the very late K types (K6–K8 III), for example, based on α Lyncis (K7 III) rather than relying on our K5 III template, but very few of these stars are to be found in the Walker-Cohen atlas.

To augment the sample of 422 stars, we might choose different approaches. In the first, we might seek to construct new composites for the missing types, notably for K4 III, and the mid to late G types (G7–G8–G9 III). In the absence of the Kuiper Airborne Observatory, spectral fragments for these new composites might be available only from space-based spectrometers, e.g., the *ISO* SWS or PHT-P and PHT-S. Precision photometry might then be sought, or reliance again placed on *IRAS* measurements, so that the range from G6.5 to G9 III and all the K4 III's could be templated. Such an extension would provide an additional maximum of 104 stars (49 late G giants and 55 K4). We note, however, the worldwide flight from maintaining conventional (single detector) infrared photometers at many major observatories. We commend those few institutions that have staunchly continued to offer bolometers and/or InSb systems and sincerely hope that they will not be encouraged to dismiss these as redundant solely because of the plethora of infrared cameras available. "True photometry" will always have a role. It is yet to be demonstrated that cameras and their associated software are capable of the same stable, high-quality radiometry achieved by careful workers with single detectors and significant focal-plane apertures.

M. C. and R. G. W. gratefully acknowledge the support for these calibration efforts through Phillips Laboratory (now the Air Force Research Laboratory) by Stephan Price on contract F19628-92-C-0900. It is a pleasure to thank our many colleagues who aided our efforts by supplying filter transmission profiles and pursuing questions of exactly which filters were in what photometers at specific times, notably Bob Gehrz, Terry Jones, Ian Glass, Chick Woodward, Dick Joyce, Harry Hyland, and Patrice Bouchet. We thank Andrew McWilliam for providing such detailed documentation for the McWilliam-Lambert narrowband photometry. M. C. also thanks his colleagues on the *ISO* Calibration Working Group for their ongoing encouragement and support for this work, principally Andrea Moneti and Michel Breitfellner. K. N. thanks the staff of Institute of Space and Astronautical Science (Japan) and also the staff of Beijing Astronomical Observatory, and the United Laboratory of Optical Astronomy, Chinese Academy of Sciences, for their kind support of his observations. This research has made use of the SIMBAD database, operated at CDS, Strasbourg, France.

APPENDIX

STELLAR NEAR-INFRARED PHOTOMETRY

Tables A1, A2, A3, A4, and A5 contain the new photometry acquired by B. C., P. H., M. K., and K. N.

TABLE A1

PHOTOMETRY ACQUIRED FROM SAAO (B. C.)

Star	J	H	K	L'	σ_J	σ_H	σ_K	$\sigma_{L'}$
HR 3	2.879	2.280	2.202	2.141		Carter standard		
HR 37	2.695	1.866	1.724	1.585	5	2	8	3
HR 74	1.661	1.022	0.923	0.825	8	7	8	9
HD 1879	3.311	2.413	2.244	2.088	8	11	5	8
HR 98	1.733	1.376	1.334	1.322		Carter standard		
HR 99	0.544	−0.107	−0.192	−0.293	4	3	4	8
HR 117.....	2.901	2.052	1.895	1.729		Carter standard		
HR 188.....	0.401	−0.138	−0.224	−0.306		Carter standard		
HR 201.....	3.179	2.256	2.092	1.948	4	9	10	1
HR 322.....	1.842	1.348	1.279	1.207		Carter standard		
HR 334.....	1.622	0.985	0.886	0.779		Carter standard		
HR 400.....	2.829	1.924	1.763	1.611	4	5	12	5
HR 402.....	1.870	1.271	1.189	1.113	10	6	8	4
HR 440.....	2.292	1.720	1.653	1.564	4	8	3	10
HD 9692	3.620	2.672	2.494	2.346	5	7	10	11
HR 539.....	1.933	1.314	1.224	1.129				
HR 602.....	2.497	1.667	1.519	1.391	5	3	5	12
HR 688.....	3.040	2.171	2.019	1.880	7	2	8	4
HR 759.....	2.380	1.493	1.310	1.164	10	7	5	5
HD 20356.....	3.475	2.561	2.400	2.294	10	8	9	8
HR 1106	2.792	1.170	2.076	2.020	7	4	7	9
HR 1136	2.006	1.490	1.420	1.402		Carter standard		
HR 1231	0.119	−0.780	−0.939	−1.052	8	3	7	6
HR 1318	2.998	2.354	2.266	2.172		Carter standard		
HR 1326	2.058	1.434	1.349	1.281		Carter standard		
HR 1393	1.462	0.642	0.506	0.403	6	4	4	9
HR 1453	2.842	2.279	2.202	2.161		Carter standard		
HR 1481	2.057	1.431	1.344	1.281	4	3	7	12
HR 1654	0.736	−0.067	−0.204	−0.322		Carter standard		
HR 2065	2.883	1.990	1.838	1.714	11	3	9	3
HR 2131	2.773	1.922	1.760	1.632	10	4	7	7
HR 2326	−1.179	−1.310	−1.333	−1.386	8	4	6	1
HR 2491	−1.385	−1.382	−1.367	−1.370	13	6	4	20
HR 2574	1.620	0.796	0.672	0.537		Carter standard		
HR 3425	3.099	2.187	1.997	1.837	5	5	13	3
HR 3480	3.293	2.418	2.235	2.112	11	5	5	7
HR 3518	1.913	1.208	1.102	1.003	6	3	5	7
HR 3535	2.810	1.931	1.752	1.621	2	6	2	11
HR 3628	1.872	0.994	0.839	0.709	6	3	3	4
HR 3738	3.058	2.213	2.068	1.943	10	12	6	7
HR 3748	−0.319	−1.078	−1.221	−1.339	12	15	16	4
HR 3802	3.384	2.537	2.406	2.287	10	8	3	14
HR 3803	0.456	−0.407	−0.562	−0.687	7	3	7	4
HR 4050	0.932	0.170	0.026	−0.123	6	10	7	6
HR 4063	2.044	1.267	1.113	0.951	3	4	6	11
HR 4080	3.042	2.455	2.365	2.272	4	3	1	10
HR 4094	1.312	0.508	0.362	0.233		Carter standard		
HR 4104	1.829	1.018	0.884	0.768	6	9	9	4
HR 4145	2.326	1.455	1.296	1.175	7	2	4	8
HR 4174	1.335	0.462	0.292	0.137		Carter standard		
HR 4216	1.184	0.692	0.602	0.532		Carter standard		
HR 4232	1.067	0.366	0.266	0.147		Carter standard		
HR 4287	2.322	1.719	1.635	1.515	7	5	3	6
HR 4289	3.259	2.474	2.316	2.144	4	5	5	10
HR 4299	1.876	1.006	0.841	0.687	5	3	8	13
HR 4382	1.686	1.015	0.936	0.841		Carter standard		
HR 4396	2.464	1.636	1.487	1.343	5	6	7	13
HR 4402	2.018	1.146	0.988	0.833	9	9	11	7
HR 4432	2.196	1.334	1.194	1.061	3	4	9	9

TABLE A1—*Continued*

Star	J	H	K	L'	σ_J	σ_H	σ_K	$\sigma_{L'}$
HR 4450.....	2.017	1.514	1.437	1.339		Carter standard		
HR 4503.....	2.734	1.927	1.788	1.640	2	5	4	8
HR 4526.....	2.464	1.536	1.371	1.213	3	4	3	3
HR 4786.....	1.220	0.759	0.692	0.608		Carter standard		
HR 4831.....	2.929	2.358	2.263	2.150	3	5	4	6
HR 4888.....	2.099	1.362	1.236	1.109	5	8	1	11
HR 4906.....	2.341	1.461	1.266	1.068	7	5	8	9
HR 5020.....	1.513	1.026	0.952	0.883		Carter standard		
HR 5064.....	2.611	1.765	1.615	1.468	4	2	6	13
HR 5068.....	3.045	2.486	2.393	2.301	6	5	7	11
HR 5152.....	3.316	2.383	2.203	2.046	5	5	5	5
HR 5287.....	1.410	0.772	0.684	0.595		Carter standard		
HR 5288.....	0.388	−0.178	−0.260	−0.361		Carter standard		
HR 5315.....	1.913	1.118	1.004	0.885		Carter standard		
HR 5410.....	2.893	2.055	1.916	1.772	8	5	6	8
HR 5513.....	3.199	2.328	2.156	2.000	2	3	6	1
HR 5526.....	2.015	1.188	1.068	0.951	7	5	3	13
HR 5590.....	2.440	1.489	1.311	1.156	9	8	6	9
HR 5615.....	3.262	2.369	2.187	2.028	3	6	8	7
HR 5622.....	2.479	1.631	1.472	1.325	5	5	8	8
HR 5705.....	0.948	0.097	−0.048	−0.181	11	8	10	11
HR 5743.....	2.986	2.135	1.983	1.852	3	5	4	6
HR 5794.....	1.335	0.577	0.455	0.337	6	8	6	5
HR 5797.....	1.974	1.206	1.073	0.955	6	1	7	5
HR 6056.....	−0.177	−1.061	−1.228	−1.345	6	7	7	6
HR 6075.....	1.635	1.090	1.012	0.971	6	11	10	10
HR 6166.....	1.388	0.528	0.368	0.247	9	12	16	2
HR 6217.....	−0.339	−1.077	−1.206	−1.336	11	5	8	8
HR 6229.....	1.022	0.145	−0.009	−0.123	7	5	4	5
HR 6241.....	0.440	−0.183	−0.273	−0.363		Carter standard		
HR 6417.....	2.758	2.072	1.972	1.889	4	2	4	10
HR 6553.....	1.050	0.809	0.765	0.734	8	11	14	2
HR 6682.....	1.818	0.904	0.728	0.599	7	10	10	4
HR 6855.....	1.855	1.012	0.871	0.773	6	8	3	8
HR 6869.....	1.652	1.094	1.024	0.989	8	13	10	5
HR 6913.....	1.082	0.482	0.396	0.340	5	10	10	7
HR 7092.....	2.560	1.649	1.482	1.352	5	7	8	3
HR 7150.....	1.640	1.014	0.915	0.827		Carter standard		
HR 7234.....	1.358	0.686	0.588	0.497		Carter standard		
HR 7259.....	2.201	1.588	1.485	1.369	5	3	3	8
HR 7323.....	3.436	2.505	2.325	2.181	4	3	8	7
HD 187150.....	3.423	2.494	2.316	2.183	4	6	7	6
HR 7559.....	3.404	2.570	2.413	2.300	6	4	6	7
HR 7584.....	2.832	1.928	1.760	1.624	8	7	7	6
HR 7604.....	2.168	1.418	1.284	1.157	5	2	5	11
HR 7652.....	2.424	1.646	1.519	1.407	5	6	6	3
HR 7659.....	2.875	2.130	2.030	1.939	5	4	2	3
HR 7754.....	2.030	1.520	1.447	1.397		Carter standard		
HR 7869.....	1.464	0.904	0.823	0.746		Carter standard		
HR 7873.....	2.180	1.294	1.149	1.028	7	7	2	1
HR 7909.....	2.768	1.933	1.757	1.608	3	4	5	10
HR 7952.....	2.280	1.434	1.290	1.176	4	5	9	5
HR 7980.....	1.249	0.365	0.202	0.057		Carter standard		
HR 8015.....	3.006	2.210	2.065	1.942	2	7	6	10
HR 8080.....	1.583	0.712	0.540	0.399	5	6	2	7
HR 8411.....	2.270	1.559	1.437	1.324	3	7	9	3
HR 8502.....	0.600	−0.162	−0.289	−0.399	5	5	3	5
HR 8679.....	1.239	0.384	0.222	0.096	6	2	2	4
HR 8685.....	3.082	2.308	2.183	2.068	10	8	5	8
HR 8774.....	2.809	1.989	1.840	1.736	3	5	6	10
HR 8820.....	2.301	1.777	1.692	1.623	6	5	4	2
HR 8841.....	2.480	1.877	1.794	1.720	6	2	5	6
HR 8863.....	2.611	1.994	1.908	1.816	3	4	3	10
HR 8898.....	2.913	2.048	1.880	1.739	9	4	2	3
HR 9073.....	2.795	1.927	1.765	1.631	7	5	6	7

NOTE.—Individual standard deviations (in mmag) follow the magnitudes.

TABLE A2

BROADBAND PHOTOMETRY ACQUIRED FROM TENERIFE (P. H.)

Star	J	σ_J	H	σ_H	K	σ_K	L'	$\sigma_{L'}$
HR 7001.....	−0.001	0.005	0.000	0.005	−0.001	0.005	0.001	0.007
HR 337	−0.962	0.006	−1.756	0.006	−1.942	0.005	−2.009	0.001
HR 1457.....	−1.938	0.015	−2.649	0.005	−2.854	0.008	−2.986	0.003
HR 2491.....	−1.411	0.005	−1.385	0.005	−1.388	0.010	…	…
HR 2990.....	−0.576	0.007	−1.024	0.007	−1.116	0.007	…	…
HR 5340.....	−2.249	0.007	−2.878	0.005	−2.992	0.011	−3.124	0.006
HR 6705.....	−0.433	0.005	−1.148	0.005	−1.309	0.005	−1.442	0.008
HR 8775.....	−1.255	0.007	−2.112	0.013	−2.333	0.008	−2.414	0.004
HR 80	3.092	0.009	2.423	0.010	2.285	0.010	2.190	0.014
HR 168	0.316	0.011	−0.208	0.005	−0.327	0.005	…	…
HR 253	2.788	0.026	2.165	0.005	2.059	0.005	1.981	0.006
HR 434	2.376	0.022	1.676	0.013	1.530	0.012	…	…
HR 464	1.571	0.010	…	…	…	…	0.653	0.002
HR 489	2.148	0.005	1.492	0.034	1.297	0.007	1.144	0.010
HR 500	…	…	…	…	…	…	1.868	0.006
HR 617	…	…	…	…	…	…	−0.743	0.006
HR 648	2.758	0.008	1.998	0.007	1.810	0.007	2.015	0.026
HR 940	3.253	0.007	2.484	0.007	2.299	0.008	2.184	0.016
HR 941	2.138	0.007	1.695	0.007	1.596	0.007	…	…
HR 947	2.711	0.007	2.197	0.007	2.093	0.007	1.423	0.011
HR 999	…	…	…	…	…	…	0.717	0.009
HR 1015.....	…	…	…	…	…	…	2.165	0.006
HR 1373.....	2.124	0.007	1.702	0.007	1.596	0.007	…	…
HR 1866.....	2.645	0.007	1.865	0.007	1.671	0.007	…	…
HR 1907.....	2.285	0.007	1.780	0.007	1.692	0.007	…	…
HR 2077.....	1.994	0.007	1.520	0.007	1.428	0.007	…	…
HR 2427.....	2.734	0.007	2.178	0.007	2.060	0.007	…	…
HR 2491.....	−1.411	0.005	−1.385	0.005	−1.388	0.010	…	…
HR 2663.....	3.072	0.008	2.348	0.007	2.186	0.006	…	…
HR 2795.....	2.294	0.007	1.581	0.007	1.399	0.007	…	…
HR 2905.....	1.172	0.007	0.442	0.007	0.265	0.006	…	…
HR 2935.....	2.730	0.007	1.963	0.006	1.785	0.006	…	…
HR 3669.....	3.096	0.006	2.445	0.008	2.320	0.010	…	…
HR 4246.....	2.811	0.015	2.162	0.010	2.042	0.009	…	…
HR 4377.....	1.096	0.024	0.411	0.017	0.282	0.020	…	…
HR 4518.....	1.602	0.010	1.010	0.005	0.908	0.005	0.818	0.008
HR 4737.....	2.470	0.008	1.977	0.005	1.881	0.005	…	…
HR 4813.....	2.669	0.016	2.139	0.013	2.024	0.011	…	…
HR 4851.....	2.805	0.005	2.146	0.005	2.023	0.005	…	…
HR 5013.....	3.053	0.013	2.436	0.009	2.310	0.006	0.236	0.004
HR 5219.....	…	…	…	…	…	…	−0.089	0.003
HR 5247.....	2.503	0.005	1.800	0.005	1.653	0.005	…	…
HR 5370.....	2.782	0.012	2.246	0.009	2.131	0.005	…	…
HR 5429.....	1.363	0.011	0.736	0.005	0.618	0.005	0.520	0.004
HR 5464.....	3.089	0.007	2.310	0.011	2.170	0.005	…	…
HR 5744.....	1.322	0.005	0.776	0.005	0.675	0.005	0.584	0.010
HR 5763.....	2.132	0.009	1.369	0.006	1.197	0.005	…	…
HR 5854.....	0.696	0.005	0.183	0.006	0.080	0.010	…	…
HR 5879.....	1.045	0.005	0.242	0.010	0.064	0.017	…	…
HR 5924.....	2.469	0.010	1.700	0.011	1.529	0.005	…	…
HR 5947.....	2.012	0.005	1.405	0.005	1.293	0.005	1.218	0.004
HR 5957.....	2.887	0.005	2.135	0.005	1.980	0.005	…	…
HR 5981.....	3.264	0.008	2.520	0.005	2.371	0.014	…	…
HR 6047.....	2.884	0.005	2.187	0.005	2.037	0.009	…	…
HR 6048.....	2.817	0.007	2.153	0.005	2.022	0.007	…	…
HR 6132.....	1.236	0.029	0.746	0.024	0.651	0.022	1.864	0.008
HR 6154.....	2.781	0.008	2.033	0.005	1.853	0.006	…	…
HR 6228.....	2.342	0.005	1.624	0.008	1.443	0.007	…	…
HR 6299.....	1.259	0.005	0.730	0.005	0.528	0.005	0.554	0.003
HR 6388.....	2.877	0.020	2.248	0.008	2.129	0.006	2.010	0.013
HR 6418.....	0.776	0.006	0.114	0.005	−0.024	0.005	−0.148	0.005
HR 6464.....	2.625	0.007	1.845	0.006	1.702	0.013	…	…
HR 6498.....	1.781	0.005	1.130	0.005	0.975	0.005	0.854	0.008

TABLE A2—*Continued*

Star	J	σ_J	H	σ_H	K	σ_K	L'	$\sigma_{L'}$
HR 6526.....	1.967	0.009	1.293	0.006	1.153	0.005	1.056	0.011
HR 6556.....	1.728	0.005	1.654	0.005	1.639	0.005	...	...
HR 6603.....	0.825	0.009	0.311	0.007	0.192	0.008	0.115	0.008
HR 6623.....	2.125	0.005	1.812	0.005	1.746	0.008	...	...
HR 6688.....	1.738	0.011	1.172	0.008	1.056	0.005	0.968	0.004
HR 6695.....	1.735	0.008	1.169	0.006	1.040	0.005	...	...
HR 6872.....	2.379	0.005	1.847	0.005	1.739	0.005	1.646	0.010
HR 6895.....	1.801	0.005	1.226	0.005	1.115	0.008	1.044	0.010
HR 7064.....	2.770	0.005	2.187	0.005	2.073	0.005	1.991	0.006
HR 7192.....	2.520	0.005	1.859	0.005	1.711	0.005	1.592	0.010
HR 7328.....	2.141	0.020	1.707	0.017	1.624	0.016	...	...
HR 7429.....	2.430	0.005	1.875	0.005	1.759	0.005	1.677	0.017
HR 7525.....	0.217	0.006	−0.466	0.005	−0.631	0.005	−0.750	0.006
HR 7557.....	0.316	0.006	0.210	0.005	0.191	0.008	0.184	0.008
HR 7576.....	2.882	0.008	2.331	0.005	2.194	0.005	...	...
HR 7633.....	2.259	0.005	1.496	0.013	1.337	0.005	1.170	0.009
HR 7635.....	0.668	0.005	−0.063	0.008	−0.230	0.014	−0.353	0.005
HR 7742.....	3.211	0.020	2.486	0.009	2.339	0.023	...	...
HR 7949.....	0.673	0.009	0.160	0.005	0.065	0.009	0.021	0.004
HR 7956.....	2.700	0.005	2.086	0.005	1.956	0.005	1.875	0.008
HR 7957.....	1.785	0.007	1.344	0.005	1.245	0.005	...	...
HR 8005.....	2.709	0.007	1.943	0.007	1.785	0.009	...	...
HR 8032.....	2.848	0.005	2.173	0.005	2.025	0.006	1.925	0.016
HR 8066.....	2.740	0.006	2.011	0.014	1.829	0.013	1.636	0.016
HR 8287.....	3.195	0.016	2.489	0.008	2.340	0.014	2.221	0.009
HR 8632.....	2.240	0.008	1.596	0.008	1.471	0.009	1.375	0.018
HR 8699.....	2.023	0.008	1.277	0.007	1.094	0.007	0.994	0.004
HR 8804.....	2.860	0.007	2.206	0.007	2.047	0.008	...	...
HR 8876.....	3.095	0.007	2.382	0.007	2.218	0.007	2.119	0.011
HR 8878.....	2.814	0.015	2.150	0.009	2.025	0.009	1.952	0.014
HR 8882.....	2.790	0.010	2.052	0.010	1.879	0.010	1.776	0.017
HR 8893.....	2.856	0.005	2.226	0.009	2.088	0.008	2.004	0.023
HR 8916.....	2.477	0.022	1.977	0.013	1.877	0.012	...	...

TABLE A3

NARROWBAND PHOTOMETRY ACQUIRED FROM TENERIFE (P. H.)

Star	Jn	σ_{Jn}	Kn	σ_{Kn}	Ln	σ_{Ln}
HR 7001.....	0.007	0.010	0.000	0.010	−0.005	0.010
HR 337.....	−0.910	0.020	−1.930	0.010	−2.060	0.010
HR 1457.....	−1.950	0.020	−2.940	0.010	−3.050	0.010
HR 2990.....	−0.590	0.005	−1.140	0.005	−1.210	0.005
HR 5340.....	−2.233	0.010	−3.075	0.010	−3.150	0.010
HR 6705.....	−0.414	0.020	−1.370	0.010	−1.460	0.030
HR 8775.....	−1.210	0.005	−2.330	0.005	−2.490	0.005
HR 1963.....	2.840	0.010	2.090	0.005	2.010	0.005
HR 4954.....	2.180	0.005	1.260	0.005	1.130	0.005
HR 5602.....	...	...	1.330	0.005	...	...
HR 5755.....	3.240	0.030	2.330	0.020	2.220	0.020
HR 5763.....	2.173	0.010	1.160	0.010	0.990	0.020
HR 5826.....	2.222	0.010	1.290	0.010	1.170	0.050
HR 5924.....	2.553	0.005	1.510	0.005	1.410	0.005
HR 5957.....	2.901	0.010	1.970	0.010	1.930	0.030
HR 5981.....	3.261	0.010	2.340	0.005	2.190	0.005
HR 6047.....	2.970	0.005	2.020	0.005	1.930	0.005
HR 6056.....	...	...	−1.330	0.005	...	...
HR 6075.....	...	...	0.980	0.005	...	...
HR 6132.....	...	...	0.620	0.005	...	...
HR 6136.....	2.899	0.040	1.980	0.020	1.880	0.050
HR 6154.....	2.773	0.005	1.880	0.005	...	...
HR 6228.....	2.402	0.010	1.400	0.010	1.310	0.030
HR 6464.....	2.653	0.005	1.650	0.005	1.480	0.005
HR 6529.....	3.120	0.010	2.240	0.020	2.120	0.040
HR 6603.....	0.862	0.005	0.190	0.005	0.060	0.005
HR 6623.....	...	...	1.740	0.005	...	...
HR 6688.....	...	...	1.020	0.005	...	...
HR 6695.....	1.733	0.030	1.025	0.010	0.960	0.020
HR 6703.....	...	...	1.570	0.005	...	...
HR 6895.....	...	...	1.100	0.005	...	...
HR 7180.....	2.841	0.010	2.220	0.005	...	...
HR 7237.....	2.802	0.030	1.840	0.030	1.700	0.030
HR 7310.....	1.338	0.010	0.740	0.010	0.690	0.060
HR 7405.....	1.503	0.010	0.460	0.005	0.380	0.005
HR 7525.....	0.250	0.020	−0.650	0.010	−0.735	0.030
HR 7557.....	0.367	0.030	0.250	0.030	0.270	0.030
HR 7595.....	2.849	0.005	2.250	0.005	2.220	0.005
HR 7633.....	2.212	0.010	1.240	0.010	1.120	0.030
HR 7742.....	3.180	0.010	2.290	0.010	2.210	0.040
HR 7754.....	1.970	0.005	1.390	0.005	...	...
HR 8499.....	2.573	0.010	2.025	0.010	1.945	0.020
HR 8684.....	1.928	0.020	1.345	0.020	1.265	0.030
HR 8916.....	2.484	0.030	1.860	0.020	1.780	0.100

TABLE A4

BROADBAND PHOTOMETRY ACQUIRED FROM TENERIFE (M. K.)

Star	J	σ_J	H	σ_H	K	σ_K	L'	$\sigma_{L'}$
HR 7001.....	−0.001	0.005	0.000	0.005	−0.001	0.005	0.002	0.005
HR 0079.....	2.762	0.022	1.982	0.010	1.798	0.011	1.674	0.044
HR 0106.....	3.096	0.010	2.351	0.012	2.182	0.013	2.084	0.044
HR 0215.....	1.917	0.026	1.403	0.028	1.322	0.031	...	...
HR 0470.....	3.286	0.010	2.511	0.012	2.337	0.013	2.239	0.044
HR 0736.....	2.459	0.008	1.761	0.009	1.604	0.010	1.510	0.031
HR 1286.....	3.173	0.014	2.534	0.015	2.390	0.021	...	...
HR 1684.....	2.406	0.010	1.706	0.012	1.542	0.013	1.419	0.044
HR 1963.....	2.828	0.021	2.222	0.017	2.103	0.022	...	...
HR 2459.....	2.367	0.005	1.699	0.005	1.537	0.006	1.409	0.044
HR 2533.....	3.109	0.011	2.444	0.012	2.298	0.011	2.169	0.036
HR 2560.....	2.826	0.005	2.418	0.005	2.327	0.005	2.281	0.008
HR 2804.....	2.916	0.005	2.180	0.014	1.989	0.008	1.834	0.044
HR 2864.....	2.457	0.026	1.883	0.028	1.735	0.028	1.638	0.027
HR 2938.....	2.022	0.037	1.260	0.036	1.100	0.015	0.979	0.036
HR 2973.....	2.216	0.037	1.712	0.031	1.586	0.028	1.553	0.027
HR 3003.....	2.196	0.010	1.471	0.012	1.302	0.013	1.189	0.044
HR 3304.....	3.138	0.005	2.487	0.005	2.347	0.005	2.255	0.005
HR 3305.....	3.056	0.010	2.366	0.012	2.212	0.013	2.054	0.044
HR 3357.....	2.336	0.010	1.621	0.012	1.422	0.015	1.259	0.044
HR 3403.....	2.520	0.006	1.948	0.006	1.855	0.005	1.796	0.023
HR 3550.....	3.045	0.010	2.424	0.005	2.271	0.006	2.129	0.044
HR 3660.....	2.501	0.011	1.766	0.012	1.602	0.013	1.464	0.044
HR 3773.....	1.526	0.010	0.816	0.012	0.647	0.013	0.479	0.044
HR 3939.....	2.892	0.005	2.202	0.013	2.038	0.011	1.899	0.044
HR 4280.....	2.922	0.011	2.212	0.022	2.049	0.018	1.924	0.044
HR 4335.....	1.118	0.027	0.518	0.028	0.405	0.028	0.363	0.027
HR 4608.....	2.438	0.005	1.970	0.005	1.888	0.005	1.771	0.012
HR 4954.....	2.131	0.011	1.468	0.013	1.318	0.015	1.200	0.028
HR 4962.....	3.236	0.011	2.543	0.013	2.393	0.014	2.260	0.028
HR 5200.....	1.256	0.013	0.548	0.013	0.398	0.015	0.260	0.028
HR 5219.....	1.131	0.011	0.328	0.013	0.123	0.014	−0.064	0.028
HR 6136.....	2.840	0.005	2.175	0.005	2.013	0.005	1.891	0.010
HR 6220.....	1.876	0.005	1.431	0.005	1.350	0.005	1.257	0.011

TABLE A5

BROADBAND PHOTOMETRY ACQUIRED FROM CHINA AND JAPAN (K. N.)

Star	Site	J	H	K	L
HR 2990	T	−0.54	−1.06	−1.16	−1.17
HR 6705	B	−0.41	−1.22	−1.34	−1.39
HR 79	B	2.83	1.92	1.72	1.57
HR 106	B	3.27	2.39	2.23	2.00
HD 5462.....	B	3.14	2.17	1.91	1.78
HR 470	B	3.30	2.46	2.31	2.09
HR 648	B	2.75	1.93	1.75	1.68
HD 14146	B	3.41	2.48	2.25	2.13
HR 736	B	2.48	1.66	1.53	1.48
HR 940	B	3.29	2.45	2.29	2.22
HR 1286	B	3.27	2.50	2.37	2.18
HD 27482	B	3.31	2.31	2.05	1.91
HR 1370	B	2.43	1.51	1.29	1.12
HR 1373	T	2.17	1.63	1.56	1.51
HR 1572	T	3.41	2.51	2.35	2.22
HR 1684	B	2.64	1.75	1.56	1.43
HR 1866	B	2.75	1.78	1.62	1.53
HR 1907	T	2.19	1.65	1.57	1.56
HR 1963	B	2.91	2.20	2.10	2.08
HR 2011	B	1.67	0.80	0.61	0.40
HR 2012	T	2.13	1.52	1.40	1.31
HR 2077	T	2.02	1.48	1.40	1.35
HR 2363	T	3.30	2.45	2.28	2.08
HR 2459	T	2.51	1.74	1.58	1.42

TABLE A5—*Continued*

Star	Site	J	H	K	L
HR 2478	T	2.52	1.88	1.78	1.66
HR 2506	T	2.63	2.03	1.95	1.82
HR 2533	B	3.25	2.44	2.28	2.19
HR 2663	T	3.14	2.27	2.13	1.99
HR 2795	T	2.32	1.53	1.34	1.23
HR 2804	T	3.00	2.09	1.93	1.70
HR 2864	T	2.48	1.77	1.64	1.51
HR 2905	T	1.26	0.44	0.27	0.09
HR 2938	T	2.11	1.32	1.16	0.97
HR 2935	T	2.83	1.92	1.73	1.56
HR 2973	T	2.27	1.67	1.56	1.50
HR 3003	T	2.23	1.42	1.27	1.21
HR 3305	T	3.19	2.30	2.16	2.05
HR 3304	T	3.23	2.43	2.29	2.16
HR 3357	T	2.38	1.55	1.36	1.26
HR 3403	T	2.62	1.93	1.79	1.65
HR 3461	T	2.09	1.53	1.44	1.39
HR 3550	T	3.20	2.41	2.22	2.03
HR 3609	T	2.50	1.72	1.57	1.47
HR 3660	T	2.45	1.61	1.46	1.38
HR 3669	T	3.13	2.37	2.26	2.14
HR 3773	T	1.51	0.75	0.60	0.40
HR 3939	T	2.91	2.09	1.95	1.84
HR 4069	T	0.06	−0.77	−0.92	−1.06
HR 4247	T	1.95	1.38	1.30	1.23
HD 94336	T	3.44	2.54	2.32	2.19
HR 4280	T	2.99	2.11	1.97	1.74
HR 4335	T	1.12	0.53	0.42	0.27
HR 4371	T	2.25	1.49	1.32	1.19
HR 4434	T	0.91	−0.02	−0.21	−0.32
HR 4639	T	3.33	2.47	2.32	2.17
HR 4690	T	2.21	1.39	1.18	0.91
HR 4863	T	2.58	1.77	1.61	1.53
HR 4884	T	3.36	2.47	2.31	2.33
HR 4954	T	2.16	1.35	1.20	1.04
HR 4962	T	3.32	2.48	2.34	2.14
HR 4986	T	2.98	2.07	1.89	1.73
HR 4998	T	2.87	2.03	1.89	1.72
HR 5200	T	1.35	0.53	0.36	0.20
HR 5219	T	1.19	0.28	0.08	−0.09
HD 127093	T	2.80	1.84	1.61	1.48
HR 5755	T	3.35	2.48	2.33	2.19
HR 5763	T	2.20	1.40	1.22	0.98
HR 5826	T	2.35	1.55	1.34	1.21
HR 5924	T	2.49	1.66	1.50	1.41
HR 5957	T	3.03	2.14	1.97	1.92
HR 5981	T	3.38	2.50	2.35	2.21
HR 6047	T	3.03	2.21	2.07	2.02
HR 6154	T	2.94	2.05	1.85	1.62
HR 6228	T	2.45	1.62	1.44	1.23
HD 156652	B	3.54	2.55	2.38	2.11
HR 6464	B	2.68	1.81	1.63	1.49
HR 6695	B	1.80	1.12	1.00	0.85
HR 6728	B	2.80	1.91	1.79	1.66
HD 170951	B	3.63	2.72	2.51	2.41
HR 7237	B	2.88	1.97	1.81	1.65
HR 7302	B	2.62	1.65	1.44	1.27
HR 7405	B	1.55	0.70	0.56	0.47
HR 7514	B	3.16	2.16	1.94	1.86
HR 7633	B	2.30	1.41	1.24	1.21
HR 7635	B	0.74	−0.05	−0.22	−0.33
HR 7648	B	3.15	2.33	2.19	2.12
HR 7780	B	3.19	2.36	2.21	2.09
HR 8005	B	2.79	1.87	1.69	1.59
HR 8066	B	2.87	1.91	1.72	1.55
HR 8090	B	3.00	2.04	1.84	1.75
HR 8572	B	1.16	0.27	0.06	−0.13
HR 8699	B	2.00	1.19	1.03	0.92
HR 8804	B	3.01	2.18	2.02	1.96
HR 8882	B	2.86	2.01	1.86	1.77

NOTES.—Individual errors are not given, but typical values are J: ± 0.03; H: ± 0.04; K: ± 0.05; L: ± 0.06. Site: (T) ISAS, Tokyo, Japan; (B) Xinglong, Beijing, China.

REFERENCES

Allen, D. A., & Cragg, T. L. 1983, MNRAS 203, 777
Alonso, A., Arribas, S., & Martínez-Roger, C. 1994, A&A, 282, 684
Barlow, M. J., & Cohen, M. 1977, ApJ, 213, 737
Bessell, M. S., & Brett, J. M. 1988, PASP, 100, 1134
Bidelman, W. P. 1980, Publ. Warner Swasey Obs., 2, No. 6
Bouchet, P., Manfroid, J., & Schmider, F. X. 1991, A&AS, 91, 409
Bouchet, P., Moneti, A., Slezak, E., Le Bertre, T., & Manfroid, J. 1989, A&AS, 80, 379
Carrasco, L., Recillas-Cruz, E., García-Barreto, A., Cruz-González, I., & Serrano P. G., A. 1991, PASP, 103, 987
Carter, B. S. 1990, MNRAS, 242, 1
———. 1993, in Precision Photometry, ed. D. Kilkenny, E. Lastovica, & J. W. Menzies (Cape Town: South African Astron. Obs.), 100
Castor, J. I., & Simon, T. 1983, ApJ, 265, 304
Clark, F. O. 1996, PLEXUS Version 2.1a, CD-ROM (Hanscom AFB, MA: Phillips Lab., Dir. Geophys., Air Force Mater. Command)
Cohen, M. 1994, AJ, 107, 582
———. 1998, AJ, 115, 2092 (Paper IX)
Cohen, M., & Davies, J. K. 1995, MNRAS, 276, 715 (Paper V)
Cohen, M., Walker, R. G., Barlow, M. J., & Deacon, J. R. 1992a, AJ, 104, 1650 (Paper I)
Cohen, M., Walker, R. G., & Witteborn, F. C. 1992b, AJ, 104, 2030 (Paper II)
Cohen, M., Witteborn, F. C., Bregman, J. D., Wooden, D. H., Salama, A., & Metcalfe, L. 1996a, AJ, 112, 241 (Paper VI)
Cohen, M., Witteborn, F. C., Carbon, D. F., Augason, G., Wooden, D., Bregman, J., & Goorvitch, D. 1992c, AJ, 104, 2045 (Paper III)
Cohen, M., Witteborn, F. C., Carbon, D. F., Davies, J. K., Wooden, D. H., & Bregman, J. D. 1996b, AJ, 112, 2274 (Paper VII)
Cohen, M., Witteborn, F. C., Walker, R. G., Bregman, J. D., & Wooden, D. H. 1995, AJ, 110, 275 (Paper IV)
Di Benedetto, G. P. 1993, A&A, 270, 315
Di Benedetto, G. P., & Rabbia, Y. 1987, A&A, 188, 114
Dyck, H. M., Benson, J. A., van Belle, G. T., & Ridgway, S. T. 1996, AJ, 111, 1705
Dyck, H. M., van Belle, G. T., & Thompson, R. R. 1998, AJ, 116, 981
Engels, D., Sherwood, W. A., Wamsteker, W., & Schultz, G. V. 1981, A&AS, 45, 5
Eyer, L., & Grenon, M. 1997, in *Hipparcos* Venice '97, ed. M. A. C. Perryman & P. L. Bernacca (ESA SP-402) (Noordwijk: ESA), 467
Feast, M. W., Whitelock, P. A., & Carter, B. S. 1990, MNRAS, 247, 227
FitzGerald, M. P. 1970, A&A, 4, 234
Fluks, M. A., Plez, B., Thé, P. S., de Winter, D., Westerlund, B. E., & Steenman, H. C. 1994, A&AS, 105, 311
Frogel, J. A., Persson, S. E., Aaronson, M., & Matthews, K. 1978, ApJ, 220, 75
Gezari, D. Y., Schmitz, M., Pitts, P. S., & Mead, J. M. 1993, Catalog of Infrared Observations (NASA RP-1294) (3d ed.; Washington: NASA)
Glass, I. S. 1985, Irish Astron. J., 17, 1
———. 1993, in IAU Colloq. 136, Stellar Photometry, ed. C. J. Butler & I. Elliott (Cambridge: Cambridge Univ. Press), 154
Gould, A., & Flynn, C. 1992, A&A, 254, 105
Grasdalen, G. L., Gehrz, R. D., Hackwell, J. A., Castelaz, M., & Gullixson, C. 1983, ApJS, 53, 413
Hammersley, P. L., Jourdain de Muizon, M., Kessler, M. F., Bouchet, P., Joseph, R. D., Habing, H. J., Salama, A., & Metcalfe, L. 1998, A&AS, 128, 207
Hauser, M. G., Kelsall, T., Leisawitz, D., & Weiland, J., eds. 1997, *COBE* Diffuse Infrared Background Experiment (*DIRBE*) Explanatory Supplement (*COBE* Ref. Pub. 97-A) (version 2.1; Greenbelt, MD: GSFC), chap. 5.8.1
Hoffleit, D., & Warren, W. H., Jr. 1991, Bright Star Catalogue (NSSDC/ADC Cat. 5050) (5th rev. ed.; New Haven: Yale Univ. Obs.)
Houk, N., Cowley, A. P., & Smith-Moore, M. 1975–1988, Michigan Catalogue of Two-dimensional Spectral Types for the HD Stars (4 vols.; Ann Arbor: Dept. Astron., Univ. Mich.)
IRAS Point Source Catalog, Version 2. 1988, Joint *IRAS* Science Working Group (NSSDC/ADC Cat. 2125) (Washington: GPO) (PSC)
Jacobson, L. A. 1990, Comput. Phys., 4, 400
Johnson, H. L., Mitchell, R. I., Iriarte, B., & Wisniewski, W. Z. 1966, Commun. Lunar Planet. Lab., 4, 99
Keenan, P. C., & McNeil, R. C. 1989, ApJS, 71, 245
Kessler, M. F., et al. 1996, A&A, 27, L315
Koornneef, J. 1983a, A&AS, 51, 489
———. 1983b, A&A, 128, 84
Manduca, A. 1979, A&AS, 36, 411
Manduca, A., Bell, R. A., & Gustafsson, B. 1977, A&A, 61, 809
Matsumoto, T., & Murakami, H. 1996, Proc. SPIE, 2817, 238
McWilliam, A. 1990, ApJS, 74, 1075
McWilliam, A., & Lambert, D. L. 1984, PASP, 96, 882
Mermilliod, J.-C. 1994, Bull. Inf. CDS, 45, 3
Mill, J. D., et al. 1994, J. Spacecr. Rockets, 31, 900
Moshir, M., et al. 1992, Explanatory Supplement to the *IRAS* Faint Source Survey, Version 2 (Pasadena: JPL)
Mozurkewich, D., et al. 1991, AJ, 101, 2207
Murakami, H., et al. 1994, ApJ, 428, 354
———. 1996, PASJ, 48, L41
Neugebauer, G., & Leighton, R. B. 1969, Two-Micron Sky Survey: A Preliminary Catalogue (NASA SP-3047) (Washington: NASA) (IRC)
Noda, M., Matsumoto, T., Matsuura, S., Noguchi, K., Tanaka, M., Lim, M. A., & Murakami, H. 1994, ApJ, 428, 363
Percy, J. R. 1993, PASP, 105, 1422
Perry, C. L., & Johnston, L. 1982, ApJS, 50, 451
Perry, C. L., Johnston, L., & Crawford, D. L. 1982, AJ, 87, 1751
Quirrenbach, A., et al. 1996, A&A, 312, 160
Ridgway, S. T., Jacoby, G. H., Joyce, R. R., Siegel, M. J., & Wells, D. C. 1982, AJ, 87, 1044
Schmitz, M., Mead, J. M., & Gezari, D. Y. 1987, Infrared Source Cross-Index (NASA RP-1182) (Washington: NASA)
Selby, M. J., Hepburn, I., Blackwell, D. E., Booth, A. J., Haddock, D. J., Arribas, S., Leggett, S. K., & Mountain, C. M. 1988, A&AS, 74, 127
Stebbins, J., & Huffer, C. M. 1930, Publ. Washburn Obs., 15, 140
Tapia, M., Neri, L., & Roth, M. 1986, Rev. Mexicana Astron. Astrofis., 13, 115
Tokunaga, A. T., Golisch, W. F., Griep, D. M., Kaminski, C. D., & Hanner, M. S. 1986, AJ, 92, 1183
van Belle, G. T., et al. 1999, AJ, 117, 521
van der Bliek, N. S., Manfroid, J., & Bouchet, P. 1996, A&AS, 119, 547
Wainscoat, R. J., Cohen, M., Volk, K., Walker, H. J., & Schwartz, D. E. 1992, ApJS, 83, 111
Walker, H. J., & Cohen, M. 1988, AJ, 95, 1801
Walker, R. G., & Cohen, M. 1992, An Atlas of Selected Calibrated Stellar Spectra (NASA CR-177604) (Moffett Field, CA: Ames Res. Cent.)